A Szilikátipari Tudományos Egyesület lapja

építőanyag

Journal of Silicate Based and Composite Materials

A TARTALOMBÓL:

2019/3

European Materials Research Society

E-MRS now has more than 4,000 members from industry, government, academia and research laboratories, who meet regularly to debate recent technological developments of functional materials. The E-MRS differs from many single-discipline professional societies by encouraging scientists, engineers and research managers to exchange information on an interdisciplinary platform, and by recognizing professional and technical excellence by promoting awards for achievement from student to senior scientist level. As an adhering body of the International Union of Materials Research Societies (IUMRS), the E-MRS enjoys and benefits from very close relationships with other Materials Research organizations elsewhere in Europe and around the world.

23 RUE DU LOESS, BP 20 - 67037
STRASBOURG CEDEX 02, FRANCE
EMRS@EUROPEAN-MRS.COM
WWW.EUROPEAN-MRS.COM

építőanyag
Journal of Silicate Based and Composite Materials
2019/3

TARTALOM

CONTENT

A finomkerámia-, üveg-, cement-, mész-, beton-, tégla- és cserép-, kő- és kavics-, tűzállóanyag-, szigetelőanyag-iparágak szakmai lapja
Scientific journal of ceramics, glass, cement, concrete, clay products, stone and gravel, insulating and fireproof materials and composites

A folyóiratot referálja · The journal is referred by:
A folyóiratban lektorált cikkek jelennek meg.
All published papers are peer-reviewed.
Kiadó · Publisher: Szilikátipari Tudományos Egyesület (SZTE)
Elnök · President: ASZTALOS István
1034 Budapest, Bécsi út 122–124.
Tel.: +36-1/201-9360 ▪ E-mail: epitoanyag@szte.org.hu
Tördelő szerkesztő · Layout editor: NÉMETH Hajnalka
Címlapfotó · Cover photo: GYURKÓ Zoltán

WWW.EPITOANYAG.ORG.HU
EN.EPITOANYAG.ORG.HU

Online ISSN: 2064-4477
Print ISSN: 0013-970x
INDEX: 2 52 50 ▪ 71 (2019) 73–104

Enhanced mechanical, thermal and barrier properties of clay-based polymer nanocomposite systems

David P. PENALOZA Jr.
is an associate professor in the Chemistry Department, College of Science, De La Salle University. His research interests focus on self-assembled systems and nanostructured materials.

David P. PENALOZA Jr. ▪ Chemistry Department, College of Science, De La Salle University, Manila, Philippines ▪ david.penaloza.jr@dlsu.edu.ph

Érkezett: 2019. 01. 09. ▪ Received: 09. 01. 2019. ▪ https://doi.org/10.14382/epitoanyag-jsbcm.2019.13

Abstract

Silicate clay-based polymer nanocomposites derived from the use of an organically modified clay montmorillonite (MMT) mineral and other related materials have attracted a great deal of technological and scientific interest owing to the promise of greatly improved properties over those of the unfilled polymer. In this review, enhancement in different properties – e.g. mechanical strength, thermal stability and flammability as well as barrier properties – of the resulting nanohybrid materials through the incorporation of a modified clay to a bulk polymer - is discussed.

Keywords: clay-polymer nanocomposites, property enhancement, modified clay
Kulcsszavak: agyag-polimer nanokompozitok, tulajdonságjavítás, módosított agyag

1. Introduction

Clay-polymer hybrid materials are a class of inorganic-organic hybrids having a polymeric material reinforced with a small loading (<10%) of clay fillers [1-10]. The term nanocomposite refers to a combination of two or more materials where one of the phases has one, two or three dimensions within the nanometer (10^{-9} m) range [11]. Due to the small size and the high surface-to-volume ratio of the inorganic filler at this length scale, the polymer nanocomposites have exhibited remarkable property enhancements and new properties compared to their unfilled polymer and conventional composites.

Two important research outputs have contributed immensely in the increased attention in the field of polymer nanocomposites. First is the pioneering work of Toyota in the late 1980s where silicate-based nanocomposite was prepared from a polyamide by scientists from the Toyota's Central Research and Development Laboratories (CRDL) [12-18]. The researchers were able to synthesize nylon-clay hybrids (NCHs) using in situ intercalative polymerization technique. The NCHs have exhibited substantial increases in the tensile strength, Young's modulus and heat distortion temperature. These remarkable property enhancements led to the first commercial application of clay-filled polymer in the manufacture of timing belt cover on Toyota cars. Then in 1993, the research team of Vaia et al. [19] showed that it is possible to prepare a clay-based polymer nanocomposite by melt mixing polymers with clays previously modified with cationic organic surfactants. This process eliminates the use of organic solvents. This is very appealing from the point of view of the industries as clay-based polymer-nanocomposites can be prepared using existing industrial setups. These two key studies have opened the doors for vigorous research works aimed at enhancing properties of various types of polymers in recent years [20].

2. Mechanical performance

In order to improve mechanical properties of polymers, fillers in the form of fibers, particles or platelets are incorporated in the polymer matrix to form a composite. Enhancement in properties of the resulting hybrids is exhibited even at relatively low filler content using nano-sized inorganic inclusions, such in the case of silicate platelets in clay-based polymer nanocomposites. Unlike traditional composites where as high as 50% by weight filler is needed to effect a substantial change in the mechanical properties, the incorporation of nano-sized particles, like silicate platelets, can lead to a comparable property effect even at a very low clay loading (<10% weight).

The researchers from the Toyota's Central Research and Development Laboratories were the first to demonstrate in the 1980s that a substantial increase in the mechanical properties of a polyamide resin can be realized through reinforcing the nylon matrix with a silicate clay. They successfully prepared a nylon-clay hybrid (NCH) that possessed improved mechanical and thermal properties – a higher modulus, an enhanced strength and a better heat distortion temperature – over the unfilled nylon. These property enhancements resulted in NCHs being applied to automotive timing belt covers as an engine part [14-18, 21-25].

Cho and Paul (2000) [26] compared the properties of a modified MMT filled-polyamide nanocomposite with a glass fiber-reinforced composite in studying the effect of using two different inorganic fillers in reinforcing the same polyamide matrix that the Toyota scientists used. About 38% increase in the tensile modulus was observed when the nylon 6 matrix was filled with 5% wt organoclay (3.66 GPa) compared to the unfilled nylon 6 (2.66 GPa). The same amount of glass fiber reinforcement (5% wt) gives a lower tensile modulus (3.26 MPa, 23% improvement relative to the bulk nylon). However, when 5% wt of the glass fiber was added to the 5% wt organoclay-filled nylon nanocomposite, the modulus is 81% higher (4.82 GPa) than the neat polyamide. This significant increase only

shows that a synergistic effect on the modulus was achieved when the clay-filled polyamide nanocomposite was used as the matrix to prepare a glass fiber-reinforced composite as measured value is far greater than the additive sum of the modulus of the individual nanofiller-reinforced nylons. The nanocomposites were prepared via direct melt compounding using a conventional twin screw extruder.

Various researchers have carried out research on the effect of clay additions on the structure and property of epoxies. Epoxies are important thermosetting polymers that are widely used as matrices of polymer composites, adhesives for aerospace applications and coatings for metals. For instance, Wang and Pinnavaia (1994) [27] reported enhanced mechanical properties of an epoxy system that is filled with delaminated MMT clay. The epoxide resin used is the diglycidyl ether of bisphenol A while the organoclay is an MMT clay previously modified with various ammonium alkyl halides. The epoxy resin is heated with the onium ion exchanged form of the MMT in the presence of diamine curing agent. The long-chain alkyl surfactants facilitate the insertion of the epoxy monomer in the clay galleries promoting the epoxide polymerization between platelets. They found that the length of the intercalating agent affects the final morphology of the clay filler. For instance, the nanocomposites formed from the incorporation of a MMT clay modified with $CH_3(CH_2)_7NH_3^+$, $CH_3(CH_2)_{11}NH_3^+$ and $CH_3(CH_2)_{15}NH_3^+$ yield exfoliated nanocomposite as shown by the absence of the d_{001} spacing in their XRD plots. The use of shorter alkyl ammonium cations produced intercalated structure.

The mechanical properties of this hybrid have remarkably improved compared to the neat epoxy. For example, the tensile strength and modulus of the epoxy system filled with $CH_3(CH_2)_{17}$-NH_3^+-MMT increases with an increasing clay reinforcement. At the addition of only 15 wt % of the exfoliated organoclay, more than a ten-fold increase in the strength and modulus compared to the unfilled epoxy. Also, the strain at break for the prepared epoxy-clay composites remains the same as the pristine matrix suggesting that the clay filler nanoparticles do not disrupt continuity of the epoxy matrix.

The organoclay incorporation is also found effective in reinforcing polyurethanes [28-31]. Wang and Pinnavaia (1998) [32] reported an increase in the strength and toughness of a polyurethane nanocomposite enhanced with an MMT organoclay. A polyurethane matrix was filled with a modified MMT clay. Initially, the MMT was derivatized by replacing the exchangeable cations of the native mineral with the more organophillic alkyl ammonium ions, $C_{18}H_{37}NH_3^+$. At a loading of only 10 wt % of the organoclay, the strength and modulus of the nanocomposites are more than doubled while also increasing the strain-at-break. Another group, Wei et al. (2000) [33] also reported improved mechanical properties for the PU-MMT nanocomposites prepared via in situ polymerization. The addition of only 1 wt% of MMT clay modified with tris(hydroxymethyl)aminomethane to a PU matrix results in a 34% increase in Young's modulus, a 1.7-times increase in tensile strength and a 1.3-fold increase in the elongation at break of the PU-MMT nanocomposite. Song et al. (2003) [34] noted enhanced tensile strength (120% increase) and doubled elongation at break when MMT clay was added to a PU matrix.

These property enhancements were found to be dependent on the silicate content of the nanocomposite. The common observation in the mechanical property measurements of the polymer nanocomposites enhanced with clay fillers is that it is very unusual to improve modulus and strength while at the same time significantly improving toughness of the bulk material [35]. The enhancement in strength and modulus is directly attributable to the reinforcement provided by the dispersed silicate nanolayers. The authors suggested that the improved elasticity that they observed for their nanocomposite may be attributed in part to the plasticizing effect of the gallery onium ions that are used to previously modify the silicate fillers prior to their incorporation in the polymer matrix.

The remarkable mechanical property improvements of the nanocomposites like significantly enhanced stiffness and tensile strength observed through the clay incorporation in engineering plastics have attracted interest in the use of silicate clays to improve some physical attributes of thermoplastic olefins [36-37]. To improve their properties, the nanocomposites derived from the incorporation of silicate clays onto these poly(olefins) have been studied [38-41]. Two examples of widely used commodity thermoplastic olefins are poly(propylene) and poly(ethylene).

Hasegawa and co-workers (1998) [37] prepared clay-based polypopylene nanocomposites using a maleic anhydride-modified PP oligomer (PP–MA) as a compatibilizer. The polymer matrix was melt-blended with a silicate clay that was previously treated with the compatibilizer. Remarkable mechanical property enhancements were noted in the nanocomposites. The dynamic storage moduli of the nanocomposites were higher than that of the unmodified poly(propylene) up to 130 °C. The modulus of the nanocomposite containing 5 wt % clay and 22 wt % PP–MA nearly doubled compared to that of plain poly(propylene) at 80 °C. As the dispersibility of the clays was improved, the reinforcement effect of the clays was also increased. The authors noted that the clay particles became smaller and were dispersed more uniformly, as the ratio of compatibilizer to the clay was increased.

Parent and co-researchers (2002) [42] observed significant property enhancement in the Young's modulus of exfoliated clay-based poly(ethylene) nanocomposites compared to the unfilled poly(ethylene). The nanocomposites containing 5 wt% and 10% Nanomer I.44PA led to an increase of 30% (220 MPa) and 53% (258 MPa), respectively compared to the neat poly(ethylene) (183 MPa). The anhydride-modified poly(ethylene) (PE-g-MAn) has a Young's modulus of 169 MPa. The nanocomposites were prepared by melt compounding a commercial organoclay Nanomer 1.44PA (Nanocor Inc.) that is ion-exchanged with a dimethyldialkylammonium halide (70% C_{18}, 26% C_{16} and 4% C_{14}) in a matrix of graft-modified poly(ethylene) (PE-g-MAn, Fusabond® M611-25, DuPont Canada, MFI=9.6). PE-g-MAn contains approximately 1% wt of maleic anhydride as modifier.

Based on their studies of melt compounding various pre-treated organoclay into a matrix of linear low density poly(ethylene) to prepare clay-based polymer nanocomposites, Hotta and Paul (2004) [43] observed that in some cases, a small

clay loading (about 5%) resulted to doubling of the modulus. The morphological studies of these nanocomposites using WAXD and TEM revealed the clay was largely exfoliated.

The above mentioned improvements in the mechanical properties of nanocomposites have attracted attention for the use of these materials in various automotive and industrial applications. These include their use in the car industry as mirror housings, engine and timing belt covers, door handles and intake manifold. They are also being currently considered in the manufacture of parts for general use equipment as housings for power tools, impellers and blades for vacuum cleaners and covers for portable electronic equipment.

3. Thermal stability and flammability

It has been reported that the MMT clay when used as fillers can be used to enhance thermal stability and reduce flammability of some polymers.

Burnside and Giannelis (1995)[44] reported a clay-based poly(dimethylsiloxane) (PDMS) nanocomposite that is significantly more thermally stable compared to a neat PDMS polymer. The nanocomposite was prepared by sonicating a silanol-terminated PDMS (18,000 g/mole) with MMT, that is ion exchanged with a dimethyl ditallow ammonium salt. A tallow is a naturally-occurring hydrocarbon that contains a mixture of various lengths of alkyl chains (C_{18} - 65 wt%, C_{16} - 30 wt% and C_{14} - 5 wt%). The nanocomposite contains only 10% mass fraction of the modified clay. At 50% weight loss (*Fig. 1*), the nanocomposite has displayed more than 140 °C increase in its degradation temperature than the unfilled PDMS. The increased thermal stability was attributed by the authors to the hindered diffusion of volatile decomposition products from the nanocomposite. X-ray diffraction showed that the clay filler was exfoliated as the nanocomposite had a featureless X-ray pattern indicating a disordered–delaminated nanostructure.

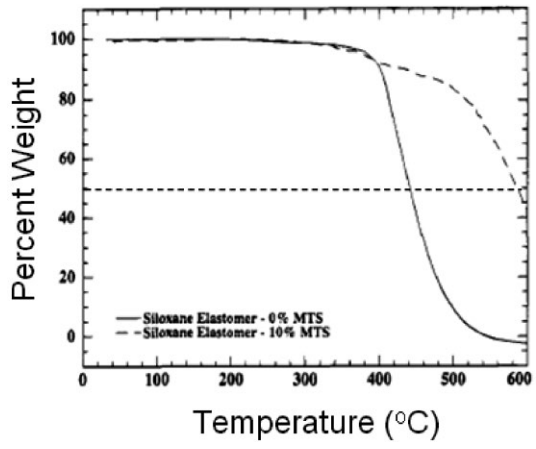

Fig. 1. A nanocomposite prepared by incorporating well dispersed MMT clay platelets in a poly(dimethysiloxane) (PDMS) matrix exhibited a substantial increase in its degradation temperature by as much as 140 °C at 50 % weight loss compared to an unfilled PDMS polymer as shown in this TGA thermogram [44]

1. ábra A diszpergált MMT-agyaglemezek poli(dimetil-sziloxán) (PDMS) mátrixba való beépítésével előállított nanokompozit jelentősen megnövelte a lebomlási hőmérsékletet (akár 140 °C-kal, 50% -os tömegveszteségnél), normál PDMS polimerhez képest, amint azt a TGA ábra mutatja [44]

Using melt intercalation, a poly(ester) nanocomposite was prepared by incorporating an MMT clay that is previously ion exchanged with an ammonium tallow. The nanocomposite obtained using poly(butylene terephthalate) (PBT) containing 3% telechelic ionic groups dispersed with 5% of the organoclay exhibited improved thermal characteristics. It has a heat distortion temperature (HDT) that is 48 °C higher compared to that of the unfilled PBT. Also, the thermogravimetric analysis revealed higher heat decomposition temperature of the nanocomposite compared to the neat poly(ester) [45].

Clay-based polymer nanocomposites were also found to exhibit a substantial increase in the flame retardancy relative to the bare polymer. The flame retardancy effect appears to originate from the ability of the clay to promote char formation. The char layer acts as a barrier that slows down the heat transfer and retards the movement of gases to feed the flame [46].

The presence of nanosized silicate clays was found to promote char formation as confirmed by several studies. Vaia et al. (1999) [47] on poly(amide)-silicate nanocomposites showed increased yield in the amount of carbonaceous char when silicate clays are added. This observation of the ability of clay to promote char formation has been verified by several authors even for polymeric systems that do not normally show tendency to form char. This was reported by Wilkie et. al (2004) [48] in the preparation of a clay-based poly(styrene) nanocomposite. The clay-poly(styrene) nanocomposite was prepared via bulk polymerization using organomodified MMT clay. Prior to the polymerization of the styrene, the clay was ion exchanged with an alkyl ammonium salt containing a C_{16} chain, N,N-dimethyl-n-hexadecyl-(4-vinylbenzyl) ammonium chloride. The nanocomposite and unfilled PBT samples were subjected to a thermogravimetric analysis to study their thermal behavior. Under thermo-oxidative conditions, while the onset degradation temperature is not significantly increased, the char content of the poly(styrene) reinforced with the modified MMT is remarkably increased from 6 to 15% wt at 400 °C. The presence of clay promotes char formation during the thermo-oxidative degradation of the polymer. The char provides a transient protective barrier to the nanocomposite in combination with the silicate clay platelets acting as barrier.

Other research works also showed similar observation: like in the case of poly(ethylene) [49] poly(propylene) [50], poly(styrene) [48], acrylonitrile-butadiene-styrene copolymer (ABS) [51] and ethylene-vinyl-acetate (EVA) copolymer [52].

The char formation is complex and involves several processes [53]. A two-step mechanism was proposed by Benson and Nogia (1979) [54] to explain the oxidation chain reactions of organic molecules during thermal degradation. The first step involves chain scission of the polymer subsequently followed by volatilization. This happens at a low temperature. At a higher temperature, oxidative dehydrogenation becomes more probable producing thermally stable aromatic charred structures due to the formation of conjugate double bond sequences. In the presence of a silicate clay as a filler in the nanocomposite, the oxidative dehydrogenation dominates as evidenced by the enhanced aromatization and reduced rate of oxidation [52, 55]. Hence, the clay induces transient char formation which only started to degrade at high temperatures.

The cone calorimeter measurement is one of the most useful bench-scale methods to characterize the flammability

properties of various clay-based polymer nanocomposites. In a cone calorimeter experiment, flammability properties like heat release rate (HRR), peak heat release rate (PHRR), time to ignition (TTI), total heat released (THR) and mass loss rate (MLR) can be determined. HRR and PHRR are two important parameters to evaluate fire safety [56]. HRR is thought of as the driving force of fire while PHRR represents the point in a fire where heat is apt to propagate further or ignite adjacent objects [56]. In studying the thermal properties of clay-polymer nanocomposites using cone calorimeter experiments, other remarkable characteristics were also noted. PHRR and HRR are reduced upon incorporation of nanosized clay [46]. The time to ignition is also slightly lowered.

4. Barrier applications

Clay-based polymer nanocomposites have also shown better barrier properties in the nanocomposites compared to their unfilled polymer counterparts due to the reduced permeability against gas and solvent permeating molecules. Well-dispersed, randomly oriented single sheets of clay in the polymer matrix hinder the permeating molecules as these individual clay sheets serve as impermeable barriers in the path of the diffusion process (*Fig. 2*). When the layers are delaminated, the effective path length for molecular diffusion is increased. The dispersed platelets of the silicate clays make the permeating gas and liquid molecules undergo a tortuous path. This "maze" of clay platelets retards the progress of the gas and liquid molecules through the polymer matrix, hence the observed reduction in permeability. The reduced gas and liquid permeability of the nanocomposites make them attractive for barrier applications e.g. membrane separation and packaging applications.

An onium-alkyl modified MMT was melt-mixed with a polyolefin. The nanocomposite was produced by a gradual dilution of the intercalated MMT edge-modified with 1-hydroxydodecane-1,1-diphosphonic acid in the melt high density poly(ethylene) until a final clay concentration of 0.3 wt% was reached. Compared to the unmodified HDPE, oxygen and water vapor permeabilities were reduced by approximately 55 and 70%, respectively [57].

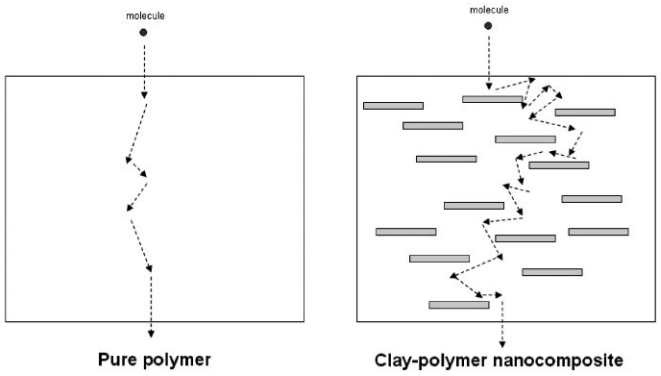

Fig. 2. Randomly well-dispersed clay platelets serve as barriers making gas molecules pass through a `torturous path' compared to unhindered path in pure polymer matrix

2. ábra A véletlenszerűen elhelyezkedő agyaglemezek gátként viselkednek és jelentősen akadályozzák a gáz molekulák egyenletes átáramlását, ahogy az a tiszta polimer mátrixban megfigyelhető

Messermith and Giannelis (1995) [58] showed that the permeability of a biodegradable aliphatic polyester to water can be remarkably reduced through the incorporation of well-dispersed, delaminated silicate clay platelets. The permeability of the films of the polymer nanocomposites to water vapor is significantly decreased with increasing silicate content. At 4.8% volume silicate content, the permeability of the nanocomposite is reduced by an order of magnitude compared to the unfilled poly(e-caprolactone). The nanocomposite synthesis involves the use of a montmorillonite clay that is ion-exchanged with protonated amino acids. The acid groups initiated the ring opening polymerization (ROP) of the heterocyclic monomer to prepare the clay-poly(e-caprolactone) nanocomposites, resulting in polymer chains that are ionically anchored to the silicate layers. The gallery polymerization was believed to promote the delamination/dispersion of the host layers during the ring-opening polymerization of the e-caprolactone monomer. X-ray diffraction patterns for the derived nanocomposites exhibit no (001) reflections due to the clay fillers suggesting that individual silicate layers were dispersed in the polymer matrix.

Chang and co-workers (2003) [59] studied the effect of using different kinds of organomodified silicate clays on the oxygen gas permeability of poly(lactic acid) (PLA) nanocomposites. The increasing amount of modified clays in the PLA nanocomposites prepared by melt intercalation systematically decreased the oxygen gas permeability of the nanocomposite films. At 10 wt%, the permeability value of the nanocomposites is reduced by half compared to the permeability of the unfilled PLA film regardless of the type of organically modified clay used as fillers. The authors attributed the decrease in the oxygen permeability of the nanocomposite films to the increase in the lengths of the tortuous paths posed by the individually dispersed clay nanoplatelets in the nanocomposites.

5. Conclusions

The enhancement in the physical properties, such as mechanical, thermal and barrier properties of the nanocomposites, is observed when the incorporation of an organoclay to a polymer matrix led to randomly dispersed, individually delaminated silicate platelets to prepare clay-based polymer nanocomposites. To achieve this, issues on clay filler and polymer compatibility and uniform dispersion of the clay within the polymeric matrix should be addressed.

6. Acknowledgment

The author would like to thank Prof. Thomas AP Seery of the University of Connecticut for his insightful comments during the preparation of this article.

References

[1] Penaloza, D. P. (2016): Mechanical and thermal properties of clay-poly(norbornene) nanocomposites from ruthenium alkylidene-mediated surface-initiated polymerization. *Kimika (The Journal of the Chemical Society of the Philippines)*, Vol. 27, No. 1: pp. 23-9. https://doi.org/10.26534/kimika.v27i1.22-28

[2] Cabedo, L. – Villanueva, M. P. – Lagarón, J. M. – Giménez, E. (2017): Development and characterization of unmodified kaolinite/EVOH

nanocomposites by melt compounding. *Applied Clay Science*, Vol. 135, pp. 300-306. https://doi.org/10.1016/j.clay.2016.10.008

[3] Geyer, B. – Hundshammer, T. – Röhner, S. – Lorenz, G. – Kandelbauer, A. (2014): Predicting thermal and thermo-oxidative stability of silane-modified clay minerals using thermogravimetry and isoconversional kinetic analysis. *Applied Clay Science*, Vol. 101, pp. 253-259. https://doi.org/10.1016/j.clay.2014.08.011

[4] Natkański, P. – Kuśtrowski, P. – Białas, A. – Piwowarska, Z. – Michalik, M. (2013): Thermal stability of montmorillonite polyacrylamide and polyacrylate nanocomposites and adsorption of Fe(III) ions. *Applied Clay Science*, Vol. 75-76, pp. 153-157. https://doi.org/10.1016/j.clay.2013.02.002

[5] Penaloza, D. P. – Seery, T. A. P. (2018): Silylated functionalized montmorillonite clay for nanocomposite preparation. *Journal of Silicate Based and Composite Materials*. Vol. 70, No. 5, pp. 140-145. https://doi.org/10.14382/epitoanyag-jsbcm.2018.26

[6] Giannelis, E. P. (1996): Polymer layered silicate nanocomposites. *Advanced Materials*, Vol. 8, No. 1, pp. 29-35. https://doi.org/10.1002/adma.19960080104

[7] Ogasa, T. – Takahashi, J. – Kemmochi, K. (1995): Polymer-based composite materials in general industrial fields. *Advanced Composite Materials: The Official Journal of the Japan Society of Composite Materials*, Vol. 4, No. 3, pp. 221-235. https://doi.org/10.1163/156855195X00032

[8] Ogawa, M. – Kuroda, K. (1997): Preparation of inorganic-organic nanocomposites through intercalation of organoammonium ions into layered silicates. *Bulletin of the Chemical Society of Japan*, Vol. 70, No. 11, pp. 2593-2618. https://doi.org/10.1246/bcsj.70.2593

[9] Alexandre, M. – Beyer, G. – Henrist, C. – Cloots, R. – Rulmont, A. – Jerome, R. – Dubois, P. (2001): One-pot preparation of polymer/clay Nanocomposites starting from Na^+ montmorillonite. 1. Melt intercalation of ethylene/vinyl acetate copolymer. *Chemistry of Materials*.Vol. 13, No. 11, pp. 3830-3832. https://doi.org/10.1021/cm011095m

[10] Fu, X. – Qutubuddin, S. (2001): Polymer-clay nanocomposites: exfoliation of organophilic montmorillonite nanolayers in polystyrene. *Polymer*, Vol. 42, No. 2, pp. 807-13. https://doi.org/10.1016/S0032-3861(00)00385-2

[11] Goldstein, A.N. (Ed.). (1997): Handbook of nanophase materials. CRC Press

[12] Hasegawa, N. – Okamoto, H. – Kawasumi, M. – Kato, M. – Tsukigase, A. - Usuki, A. (2000): Polyolefin-clay hybrids based on modified polyolefins and organophilic clay. *Macromolecular Materials and Engineering*. Vol. 280-281, No. 1, pp. 76-79. https://doi.org/10.1002/1439-2054(20000801)280:1<76::AID-MAME76>3.0.CO;2-%23

[13] Kawasumi, M. (2004): The discovery of polymer-clay hybrids. *Journal of Polymer Science Part A: Polymer Chemistry*. Vol. 42, No. 4, pp. 819-824. https://doi.org/10.1002/pola.10961

[14] Kojima, Y. – Usuki, A. – Kawasumi, M. – Okada, A. – Kurauchi, T. – Kamigaito, O. - Kaji, K. (1994): Fine structure of nylon–6–clay hybrid. *Journal of Polymer Science Part B-Polymer Physics*, Vol. 32, No. 4, pp. 625-30. https://doi.org/10.1002/polb.1994.090320404

[15] Usuki, A. – Kawasumi, M. – Kojima, Y. – Okada, A. – Kurauchi, T. (1995): Synthesis and Properties of Diamine-Modified Nylon 6-Clay Hybrid. *Kobunshi Ronbunshu*, Vol. 52, No. 7, pp. 440-444. https://doi.org/10.1295/koron.52.440

[16] Usuki, A. – Koiwai, A. – Kojima, Y. – Kawasumi, M. – Okada, A. – Kurauchi, T. Kamigaito, O. (1995): Interaction of nylon 6-clay surface and mechanical properties of nylon 6-clay hybrid. *Journal of Applied Polymer Science*, Vol. 55, No. 1, pp. 119-123. https://doi.org/10.1002/app.1995.070550113

[17] Yano, K. – Usuki, A. – Okada, A. (1997): Synthesis and properties of polyimide-clay hybrid films. *Journal of Polymer Science Part A: Polymer Chemistry*, Vol. 35, No. 11, pp. 2289-2894. https://doi.org/10.1002/(SICI)1099-0518(199708)35:11<2289::AID-POLA20>3.0.CO;2-9

[18] Yano, K. – Usuki, A. – Okada, A. – Kurauchi, T. – Kamigaito, O. (1993): Synthesis and properties of polyimide-clay hybrid. *Journal of Polymer Science Part A: Polymer Chemistry*, Vol. 31, No. 10, pp. 2493-2498. https://doi.org/10.1002/pola.1993.080311009

[19] Vaia, R.A. – Ishii, H. – Giannelis, E.P. (1993): Synthesis and properties of two-dimensional nanostructures by direct intercalation of polymer melts in layered silicates. *Chemistry of Materials*, Vol. 5, No. 12, pp. 1694-1696. . https://doi.org/10.1021/cm00036a004

[20] Penaloza DP. (2017): Review on the preparation, structure and property relation of clay-based polymer nanocomposites. *Kimika (The Journal of the Chemical Society of the Philippines)*, Vol. 28, No. 1, pp. 44-56. https://doi.org/10.26534/kimika.v28i1.44-56

[21] Chen, J. – Beake, B.D. – Bell, G.A. – Tait, Y. Gao, F. (2016): Investigation of the nanomechanical properties of nylon 6 and nylon 6/clay nanocomposites at sub-ambient temperatures. *Journal of Experimental Nanoscience,* Vol.11, No. 9, pp. 695-706. https://doi.org/10.1080/17458080.2015.1136847

[22] Haider, S. – Kausar, A. – Muhammad, B. (2016): Research advancement in high-performance polyamides and polyamide blends loaded with layered silicate. *Polymer - Plastics Technology and Engineering*, Vol. 55, No. 14, pp. 1536-1556. https://doi.org/10.1080/03602559.2016.1163602

[23] Khalid Saeed I. (2017): Morphological, thermal, mechanical and solvent uptake of clay/nylon 6,6 composites. *Journal of the Chilean Chemical Society*, Vol. 62, No. 3, pp. 3562-3565. http://dx.doi.org/10.4067/s0717-97072017000303562

[24] Vyas, A. – Iroh, J.O. (2016): Clay induced thermoplastic crystals in thermoset matrix: thermal, dynamic mechanical, and morphological analysis of clay/nylon-6-epoxy nanocomposites. *Polymer Composites,* Vol. 37, No. 7, pp. 2206-2217. https://doi.org/10.1002/pc.23399

[25] Xu, W. – Wu, X. - Sun W. (2016): Molecular dynamics studies on the overall compressive modulus of nylon 6/montmorillonite nanocomposites. *Advances in Mechanical Engineering*. Vol. 8, No. 11, pp. 1-8. https://doi.org/10.1177/1687814016677659

[26] Cho, J.W. – Paul, D.R. (2001): Nylon 6 nanocomposites by melt compounding. *Polymer*, Vol. 42, No. 3, pp. 1083-10894. https://doi.org/10.1016/S0032-3861(00)00380-3

[27] Lan, T. – Pinnavaia, T.J. (1994): Clay-reinforced epoxy nanocomposites. *Chemistry of Materials*, Vol. 6, No. 12, pp. 2216-2219. https://pubs.acs.org/doi/10.1021/cm00048a006

[28] Adak, B. – Butola, B.S. – Joshi, M. (2018): Effect of organoclay-type and clay-polyurethane interaction chemistry for tuning the morphology, gas barrier and mechanical properties of clay/polyurethane nanocomposites. *Applied Clay Science*, Vol. 161, pp. 343-53. https://doi.org/10.1016/j.clay.2018.04.030

[29] Ashhari, S. – Sarabi, A.A. (2017): Effects of organically modified nanoclay particles on the mechanical properties of aliphatic polyurethane/clay nanocomposite coatings. *Polymer Composites*, Vol. 38, No. 6, pp. 1167-1174. https://doi.org/10.1002/pc.23680

[30] Peng, S. – Iroh, J.O. (2016): Synthesis and characterization of crosslinked polyurethane/clay nanocomposites. *Journal of Applied Polymer Science,* Vol. 133, Issue 17), 43346. https://doi.org/10.1002/app.43346

[31] Wang, X.C. – Geng, T. – Han, J. – Liu, C.T. – Shen, C.Y. – Turng, L.S. – Yang, H.E. (2017): Effects of nanoclays on the thermal stability and flame retardancy of microcellular thermoplastic polyurethane nanocomposites. *Polymer Composites*, Vol. 39, No. S3, E1429-E1440. https://doi.org/10.1002/pc.24340

[32] Wang, Z. – Pinnavaia, T.J. (1998): Nanolayer reinforcement of elastomeric polyurethane. *Chemistry of Materials*, Vol. 10, No. 12, pp. 3769–3771. https://doi.org/10.1021/cm980448n

[33] Chen, T.K. – Tien, Y.I. – Wei, K.H. (2000): Synthesis and characterization of novel segmented polyurethane/clay nanocomposites. Vol. 41, No. 4, pp. 1345-1353. https://doi.org/10.1016/S0032-3861(99)00280-3

[34] Song, M. – Hourston, D.J. – Yao, K.J. – Tay, J.K.H. – Ansarifar, M.A. (2003): High performance nanocomposites of polyurethane elastomer and organically modified layered silicate. *Journal of Applied Polymer Science*, Vol. 90, No. 12, pp. 3239-3243. https://doi.org/10.1002/app.12979

[35] Tjong, S.C. – Meng, Y.Z. (2003): Preparation and characterization of melt-compounded polyethylene/vermiculite nanocomposites. *Journal of Polymer Science Part B: Polymer Physics*, Vol. 41, No. 13, pp. 1476-1484. https://onlinelibrary.wiley.com/doi/10.1002/polb.10497

[36] Usuki, A. – Kato, M. – Okada, A. – Kurauchi, T. (1997): Synthesis of polypropylene-clay hybrid. *Journal of Applied Polymer Science*, Vol. 63, No. 1, pp. 137-138. https://doi.org/10.1002/(SICI)1097-4628(19970103)63:1<137::AID-APP15>3.0.CO;2-2

[37] Hasegawa, N. – Kawasumi, M. – Kato, M. – Usuki, A. – Okada, A. (1998): Preparation and mechanical properties of polypropylene-clay hybrids

using a maleic anhydride-modified polypropylene oligomer. *Journal of Applied Polymer Science*, Vol. 67, No. 1, pp. 87-92. https://doi.org/10.1002/(SICI)1097-4628(19980103)67:1<87::AID-APP10>3.0.CO;2-2

[38] Maiti, P. – Nam, P.H. – Okamoto, M. – Hasegawa, N. - Usuki A. (2002): Influence of crystallization on intercalation, morphology, and mechanical properties of polypropylene/clay nanocomposites. *Macromolecules*, Vol. 35, No. 6, pp. 2042-2049. https://doi.org/10.1021/ma010852z

[39] Chiu, F.C. – Lai, S.M. – Chen, J.W. – Chu, P.H. Combined effects of clay modifications and compatibilizers on the formation and physical properties of melt-mixed polypropylene/clay nanocomposites. *Journal of Polymer Science Part B: Polymer Physics*. Vol. 42, No. 22, pp. 4139-4150. https://doi.org/10.1002/polb.20271

[40] Morawiec, J. – Pawlak, A. – Slouf, M. – Galeski, A. – Piorkowska, E. – Krasnikowa, N. (2005): Preparation and properties of compatibilized LDPE/organo-modified montmorillonite nanocomposites. *European Polymer Journal*, Vol. 41, No. 5, pp. 1115-1122. https://doi.org/10.1016/j.eurpolymj.2004.11.011

[41] Shah, R.K. – Paul, D.R. (2006): Organoclay degradation in melt processed polyethylene nanocomposites. Vol. 47, No. 11, pp. 4075-4084. https://doi.org/10.1016/j.polymer.2006.02.031

[42] Gopakumar, T.G. – Lee, J.A. – Kontopoulou, M. – Parent, J.S. (2002): Influence of clay exfoliation on the physical properties of montmorillonite/polyethylene composites. *Polymer*, Vol. 43, No. 20, pp. 5483-5491. https://doi.org/10.1016/S0032-3861(02)00403-2

[43] Hotta, S. – Paul, D.R. (2004): Nanocomposites formed from linear low density polyethylene and organoclays. *Polymer*, Vol. 45, No. 22, pp. 7639-7654. https://doi.org/10.1016/j.polymer.2004.08.059

[44] Burnside, S.D. – Giannelis, E.P. (1995): Synthesis and properties of new poly(dimethylsiloxane) nanocomposites. *Chemistry of Materials*, Vol. 7, No. 9, pp. 1597-1600. https://doi.org/10.1016/10.1021/cm00057a001

[45] Colonna, M. – Berti, C. – Binassi, E. – Fiorini, M. – Karanam, S. – Brunelle, D.J. (2010) Nanocomposite of montmorillonite with telechelic sulfonated poly(butylene terephthalate): effect of ionic groups on clay dispersion, mechanical and thermal properties. *European Polymer Journal*, Vol. 46, No. 5, pp. 918-927. https://doi.org/10.1016/j.eurpolymj.2010.02.003

[46] Powell, C.E. – Beall, G.W. (2006): Physical properties of polymer/clay nanocomposites. *Current Opinion in Solid State and Materials Science*, Vol. 10, No. 2, pp. 73-80. https://doi.org/10.1016/10.1016/j.cossms.2006.09.001

[47] Vaia, R.A. – Price, G. - Ruth P.N. – Nguyen, H.T. – Lichtenhan, J. (1999): Polymer/layered silicate nanocomposites as high performance ablative materials. *Applied Clay Science*, Vol. 15, No. 1-2, pp. 67-92. https://doi.org/10.1016/S0169-1317(99)00013-7

[48] Bourbigot, S. – Gilman, J.W. – Wilkie, C.A. (2004): Kinetic analysis of the thermal degradation of polystyrene-montmorillonite nanocomposite. *Polymer Degradation and Stability*. 2004;84(3):483-92. https://doi.org/10.1016/j.polymdegradstab.2004.01.006

[49] Zanetti, M. – Bracco, P. – Costa, L. (2004): Thermal degradation behaviour of PE/clay nanocomposites. *Polymer Degradation and Stability*, Vol. 85, No. 1, pp. 657-665. https://doi.org/10.1016/j.polymdegradstab.2004.03.005

[50] Zanetti, M. – Camino, G. – Reichert, P. – Mülhaupt, R. (2001): Thermal behaviour of poly(propylene) layered silicate nanocomposites. *Macromolecular Rapid Communications*. Vol. 22, No. 3, pp. 176-180. https://doi.org/10.1002/1521-3927(200102)22:3<176::AID-MARC176>3.0.CO;2-C

[51] Wang, S. – Hu, Y. – Lin, Z. – Gui, Z. – Wang, Z. – Chen, Z. – Fan, W. (2003): Flammability and thermal stability studies of ABS/montmorillonite nanocomposite. *Polymer International,* Vol. 52, No. 6, pp. 1045-1049. https://doi.org/10.1002/pi.1200

[52] Zanetti, M. – Camino, G. – Thomann, R. – Mülhaupt, R. (2001): Synthesis and thermal behaviour of layered silicate-EVA nanocomposites. *Polymer*, Vol. 42, No. 10, pp. 4501-4517. https://doi.org/10.1016/S0032-3861(00)00775-8

[53] Levchik, S.W. – Wilkie, C.A. (Eds.). (2000): Fire retardancy of polymeric materials. CRC Press.

[54] Benson, S.W. – Nangia, P.S. (1979): Some unresolved problems in oxidation and combustion. *Accounts of Chemical Research*, Vol. 12, No. 7, pp. 223-228. https://doi.org/10.1021/ar50139a001

[55] Zanetti, M. – Camino, G. – Thomann, R. - Mülhaupt R. (2001): Synthesis and thermal behaviour of layered silicate-EVA nanocomposites. *Polymer*, Vol. 42, No. 10, pp. 4501-4507. https://doi.org/10.1016/S0032-3861(00)00775-8

[56] Kiliaris, P. – Papaspyrides, C.D. (2010): Polymer/layered silicate (clay) nanocomposites: An overview of flame retardancy. *Progress in Polymer Science*, Vol. 35, No. 7, pp. 902-958. https://doi.org/10.1016/j.progpolymsci.2010.03.001

[57] Chaiko, D.J. (2006): Activation of organoclays and preparation of polyethylene nanocomposites. *E-Polymers*, Vol. 6, No. 1. https://doi.org/10.1515/epoly.2006.6.1.242

[58] Messersmith, P.B. – Giannelis, E.P. (1995): Synthesis and barrier properties of poly(e-caprolactone)-layered silicate nanocomposites. *Journal of Polymer Science Part A: Polymer Chemistry*, Vol. 33, No. 7, pp. 1047-1057. https://doi.org/10.1002/pola.1995.080330707

[59] Chang, J.H. – An, Y.U. – Sur, G.S. (2003): Poly(lactic acid) nanocomposites with various organoclays. I. Thermomechanical properties, morphology, and gas permeability. *Journal of Polymer Science Part B: Polymer Physics*, Vol. 41, No. 1, pp. 94-103. https://doi.org/10.1002/polb.10349

Ref.:
David P., **Penaloza** Jr.: *Enhanced mechanical, thermal and barrier properties of clay-based polymer nanocomposite systems*
Építőanyag – Journal of Silicate Based and Composite Materials, Vol. 71, No. 3 (2019), 74–79. p.
https://doi.org/10.14382/epitoanyag-jsbcm.2019.13

One-pot preparation of PS/silica hydrophobic coating by solution-casting using D-limonene as dispersing medium

Roderick Jesus Jude M. REGALADO ▪ Chemistry Department, College of Science, De La Salle University, Manila, Philippines ▪ roderick_regaladojr@dlsu.edu.ph

Emmanuel A. PUNZALAN ▪ Chemistry Department, College of Science, De La Salle University, Manila, Philippines ▪ emmanuel_punzalan@dlsu.edu.ph

David P. PENALOZA Jr. ▪ Chemistry Department, College of Science, De La Salle University, Manila, Philippines ▪ david.penaloza.jr@dlsu.edu.ph

Érkezett: 2018. 05. 14. ▪ Received: 14. 05. 2018. ▪ https://doi.org/10.14382/epitoanyag-jsbcm.2019.14

Abstract

Different polystyrene (PS) coatings were prepared and optimized by dissolving PS in D-limonene and subsequent dispersion of varying amounts of different chemically modified silica nanoparticles. Among the materials prepared, a PS coating filled with silica nanoparticles organo-modified with long alkyl carbon chains results in high hydrophobicity (120.8° as compared to bare PS coating – 67.0°) and excellent film-formation.

Keywords: PS/silica coatings, hydrophobicity, contact angle

Kulcsszavak: PS/szilícium-dioxid bevonatok, hidrofobitás, nedvesedési szög

Roderick Jesus Jude M. REGALADO graduated from De La Salle University (DLSU), Philippines with BS Biochemistry degree in 2018.

Emmanuel A. PUNZALAN is currently an MS Chemistry student at De La Salle University (DLSU), Philippines. He finished his BS Chemistry degree in 2016 from DLSU.

David P. PENALOZA Jr. is an associate professor in the Chemistry Department, College of Science, De La Salle University (DLSU). His research interests focus on self-assembled systems and nanostructured materials.

1. Introduction

Highly hydrophobic coatings have been of particular interest over the last decade due to their extensive potential applications in anti-corrosion [1,2], self-cleaning [3,4], anti-fouling [5,6], anti-icing [7,8], and drag-reducing materials in a wide range of industries. Surfaces with water contact angles of at least 90° are referred to as hydrophobic surfaces whereas surfaces with water contact angles greater than 150° are referred to as superhydrophobic surfaces [9].

PS is a versatile plastic material that has found wide applications in food packaging, laboratory wares [10-13], electronics and automobile parts [11,12], etc. Due to its low cost of production, most consumer goods come in PS packaging in one form or another. This poses a serious problem to the environment as PS is shown to be relatively stable and is hard to be degraded even after 32 years as stated in a previous study [14]. Over the years, the amount of PS waste that accumulates in landfills and oceans increases. Based on global statistics, about 14 million metric tons of PS are produced each year, and only about 15 percent of that is being recycled due to cost and processing issues as PS is cheaper to produce rather than to recycle and that recycling polystyrene requires it to be contaminant free [15-18].

As a coating material, it has poor barrier characteristics to oxygen and water vapor [19], which is necessary for coating applications. However, several researchers have shown that added with inorganic fillers like silica, PS-based coating materials result in better coating materials [20-22].

Here, we prepared hydrophobic polymer coatings filled with silica nanoparticles from solution-casting using D-limonene as the dispersing medium. Highly hydrophobic coatings based on polystyrene (PS) optimized with different types of surface-modified silica nanoparticles were prepared. In this study, one-pot method of preparation based on surface segregation phenomenon of nanoparticles on a polymer matrix was used. To make PS and silica dispersion, an environment-friendly solvent, D-limonene, was utilized. D-limonene is a natural solvent that is extracted from citrus fruits like oranges [23].

2. Experimental methods

2.1 Materials

Polystyrene (PS) (MW ~350, 000) and D-limonene (>97%) were purchased from Sigma-Aldrich Co. Three types of commercially available organo-modified nanosilica (SiO_2) particles: Aerosil R 812S, Aerosil R 816, and Aerosil R 972 were used in this study. Aerosil R 812S, Aerosil R 816, and Aerosil R 972 are silica nanoparticles chemically pre-modified with hexamethyldisilazane, hexadecylsilane, and dimethyldichlorosilane, respectively.

2.2 Preparation of PS/SiO_2 coatings

PS (5.0 g) in D-limonene (150 mL) was heated to 40 °C and stirred at 400 rpm for 2 hours. Afterwards, 30 mL each of the polystyrene dispersion was poured into four individual clean Erlenmeyer flasks, where silica nanoparticles where added to three of the flasks and then subjected to stirring. In summary, there are four treatments considered: (1) PS – control (no silica); (2) PS/AS1 - PS/Aerosil R 812S (99:1); (3) PS/AS2 - PS/Aerosil R 816(99/1), and PS/AS3 – PS/Aerosil R 972. Each dispersion was then coated onto clean glass cover slips via solution casting and allowed to dry overnight under ambient conditions. Of the three treatments containing silica nanoparticles, the sample exhibiting highest contact angle and good film formation was then optimized by having varying PS:SiO_2 ratios.

2.3 Wetting property measurement

The static water contact angle of each coated surface was determined by gently dropping 5 μL of distilled water onto the coated surface using a micropipette. Five replicates were performed for each of the measurements. A photo of the droplet was captured immediately after the droplet was placed on the surface, and the water contact angle was calculated using ImageJ Low-Bond Axisymmetric Drop Shape Analysis (LB-ADSA) [24,25].

3. Results and discussion

3.1 Preparation of PS/SiO_2 coatings

The four treatment samples: (1) PS – control (no silica); (2) PS/AS1 - PS/Aerosil R 812S (99:1); (3) PS/AS2 - PS/Aerosil R 816(99/1), and PS/AS3 – PS/Aerosil R 972 when solution-casted on glass slides.

As shown in *Fig. 1*, the PS dispersion containing no silica nanoparticles formed a transparent film. PS/AS1 and PS/AS2, both result in homogeneous dispersion of the nanosilica particles, though, not transparent as the PS film (no silica). PS/AS3 exhibited poor homogenous film-formation, as a result of the silica particles poorly dispersed within the PS matrix.

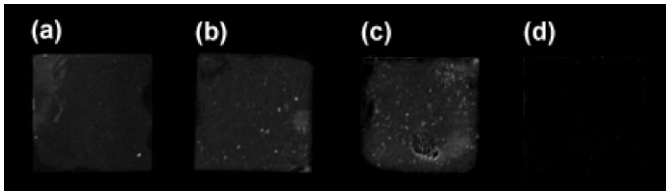

Fig. 1 Glass cover slips coated with a) PS/AS1, b) PS/AS2, c) PS/AS3 and d) PS (control)

1. ábra Üveg fedőlapok a) PS/AS1, b) PS/AS2, c) PS/AS3 és d) PS (etalon) bevonattal

The method for contact angle analysis was first calibrated by comparing the water contact angles of PS and glass used to the ones previously reported elsewhere. The average water contact angle of PS is ~68° while that of glass is ~40° [26]. Using the low-bond axisymmetric drop shape analysis (LB-ADSA) method [24,25], the water contact angles of PS and glass subtract were found to match previously documented data. As shown in *Fig. 2*, all PS films filled with nanosilica showed higher contact angle values than the bare PS coating, indicating more hydrophobic effect to the PS matrix by organo-modified silica incorporation. Though PS/AS1 results to an even coating from visual inspection than PS/AS2, the latter exhibited higher contact angle (Mean = 120.6°). Among the films with incorporated silica, PS/AS3 results in lowest contact angle value and poor dispersion of the particles. Statistical analysis of all treatments showed a significant difference in the observed contact angles of the coatings.

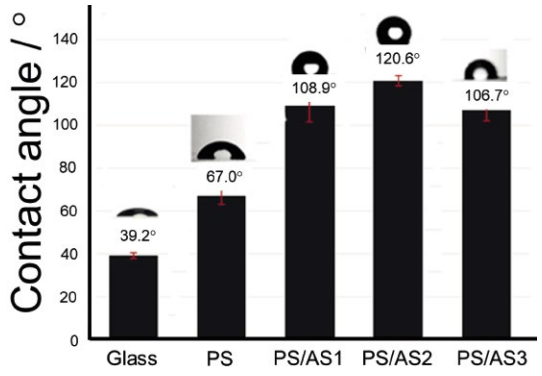

Fig. 2. Contact angle measurements of the glass substrate used and different PS coatings applied on glass

2. ábra Nedvesítési szög üvegen és különböző PS bevonatokon

From the results of film casting and contact angle measurements, PS film modified with Aerosil R 816 exhibited homogeneously dispersed particles in a PS matrix with high hydrophobicity (high contact angle). Based on an initial PS/silica ratio of 99/1, varying ratios of PS/Aerosil R816 were then prepared.

As expected, the non-wetting behavior of PS-AS2 improved with increasing concentration of modified silica (*Fig. 3*). However, at SiO_2 concentration greater than 3.0% (relative to PS) decreased hydrophobicity and poor film formation were noted due to cracking brought about by particle aggregation.

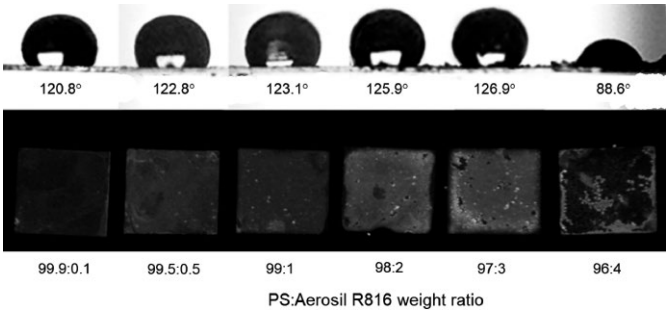

Fig. 3. Measure contact angles (upper) and photos (lower) taken of various PS films incorporated with different amounts of Aerosil R816 (PS/AS3) applied on glass

3. ábra Nedvesítési szög (felső sor) és a hozzájuk tartozó minták amelyekre különböző mennyiségű Aerosil R816 (PS/AS3) bevonatot vittek fel (alsó sor)

Fig. 4 showed PS coatings (left) filled with Aerosil R 816 (PS/AS3) at varying ratios: 99.5:0.5 and 99.9:0.1. The other two (right) correspond to glass slides coated with PS only and uncoated glass, respectively. Water droplets (colored) are applied on the surfaces to compare non-wetting behavior. Though not as clear as the unfilled PS coating, PS-filled with silica nanoparticles solution-casted using D-limonene as solvent can result in more hydrophobic coatings where optical property can be fine-tuned by changing the silica concentration.

Fig. 4. PS films incorporated with different amounts of Aerosil R816 (PS/AS3) applied on glass compared to just bare PS coating and uncoated glass slide
4. ábra Különböző mennyiségű Aerosil R816 (PS / AS3) bevonattal ellátott PS-fóliák összehasonlítva tiszta PS bevonattal és bevonat nélküli üveggel

To check on the uniformity of the prepared film from the solution casting of PS filled with Aerosil R816 (PS/AS3), at 99.9:0.1 weight ratio with D-limonene as the dispersing medium, water droplets were placed at various places across the films. As shown in *Fig. 5*, uniform water droplets can be observed displaying high contact angles, that were previously determined to have an average value of 120.8° (as opposed to the contact angle observed in PS only, 67.0°).

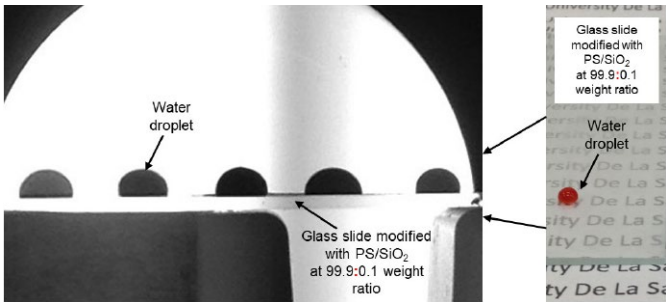

Fig. 5. Deposited water droplets deposited on the surface of PS:Aerosil R816 (PS/AS3) film (at 99.9:0.1 weight ratio) solution casted from D-limonene as solvent
5. ábra A PS: Aerosil R816 (PS / AS3) film (99,9: 0,1 tömegarányú) felületére helyezett vízcseppek

4. Conclusions

In summary, we were able to prepare a highly hydrophobic PS-based coating filled with organo-modified nanosilica particles from solution-casting using D-limonene as the dispersing medium. The film's properties such as non-wetting behavior, film-formation characteristic and optical property can be fine tuned with the type of organo-modified silica particles to be added as well as the silica concentration. From the three commercially available silica nanoparticles used: Aerosil R 812S, Aerosil R 816, and Aerosil R 972 which are silica nanoparticles chemically pre-modified with hexamethyldisilazane, hexadecylsilane, and dimethyldichlorosilane, respectively – the PS films modified with Aerosil R 816 at 0.1:99.9 weight ratio (relative to PS) result in homogeneous, highly hydrophobic (120.8°) coatings as contrasted to PS only (67.0°).

5. Acknowledgment

The authors would like to thank D&L Industries, Inc. for the technical and chemical assistance extended to carry out this study.

References

[1] Mohamed, A. M. A. - Abdullah, A. M., & Younan, N. A. (2015): Corrosion behavior of superhydrophobic surfaces: A review. *Arabian Journal of Chemistry*, Vol. 8, No. 6, pp. 749–765. https://doi.org/10.1016/j.arabjc.2014.03.006

[2] Zhan-Fang, C. - Pei, Q. - Pei, C. - Xin, W. - Guang-Yi, L., Shuai, W., - Hong, Z. (2017): Super-hydrophobic coating used in corrosion protection of metal material: review, discussion and prospects. *Metallurgical Research & Technology*, Vol. 114, No. 203, https://doi.org/10.1051/metal/2017011

[3] Syafiq, A. - Vengadaesvaran, B. - Pandey, A. K. - Rahim, N. A. (2018): Superhydrophilic smart coating for self-cleaning application on glass substrate. *Journal of Nanomaterials*, 2018, Vol. 2018, No. 6412601, pp. 1–10. https://doi.org/10.1155/2018/6412601

[4] Xue, C.-H. - Bai, X. - Jia, S.-T. (2016): Robust, self-healing superhydrophobic fabrics prepared by one-step coating of PDMS and octadecylamine. *Scientific Reports*, Vol. 6, No. 1. https://doi.org/10.1038/srep27262

[5] Cooksey, K. E. - Wigglesworth-Cooksey, B. (1992): The design of antifouling surfaces: background and some approaches. Biofilms — *Science and Technology*, pp. 529–549. https://doi.org/10.1007/978-94-011-1824-8_47

[6] Cao, S. - Wang, J. - Chen, H. - Chen, D. (2010): Progress of marine biofouling and antifouling technologies. *Chinese Science Bulletin*, Vol. 56, No. 7, pp. 598–612. https://doi.org/10.1007/s11434-010-4158-4

[7] Morita, K. - Sakaue, H. (2015): Characterization method of hydrophobic anti-icing coatings. *Review of Scientific Instruments*, Vol. 86, No. 11, pp. 86-91. https://doi.org/10.1063/1.4935585

[8] Susoff, M. - Siegmann, K. - Pfaffenroth, C. - Hirayama, M. (2013): Evaluation of icephobic coatings - screening of different coatings and influence of roughness. *Applied Surface Science*, Vol. 282, pp. 870–879. https://doi.org/10.1016/j.apsusc.2013.06.073

[9] Marmur, A. (2003): Wetting on hydrophobic rough surfaces: to be heterogeneous or not to be? *Langmuir*, Vol. 19, No. 20, pp. 8343–8348. https://doi.org/10.1021/la0344682

[10] Berruezo, M. - Ludueña, L. - Rodriguez, E. - Alvarez, V. (2013): Preparation and characterization of polystyrene/starch blends for packaging applications. *Journal of Plastic Film & Sheeting*, Vol. 30, No. 2, pp. 141–161. https://doi.org/10.1177/8756087913504581

[11] Andrady, A. L. - Neal, M. A. (2009): Applications and societal benefits of plastics. *Philosophical Transactions of the Royal Society B: Biological Sciences*, Vol. 364, No. 1526, pp. 1977–1984. https://doi.org/10.1098/rstb.2008.0304

[12] Lickly, T. D. - Lehr, K. M. - Welsh, G. C. (1995): Migration of styrene from polystyrene foam food-contact articles. *Food and Chemical Toxicology,* Vol. 33, No. 6, pp. 475–481. https://doi.org/10.1016/0278-6915(95)00009-q

[13] Wang, W. - Shi, S. - Liu, Y. - Wang, G. (2017): The application of expanded polystyrene cushion layer in oblique flexible net systems for rockfall protection: A new attempt. *International Journal of Protective Structures,* Vol. 9, No. 2, pp. 141–156. https://doi.org/10.1177/2041419617719295

[14] Otake, Y., Kobayashi, T. - Asabe, H. - Murakami, N. - Ono, K. (1995): Biodegradation of low-density polyethylene, polystyrene, polyvinyl chloride, and urea formaldehyde resin buried under soil for over 32 years. *Journal of Applied Polymer Science*, Vol. 56, No. 13, pp. 1789–1796. https://doi.org/10.1002/app.1995.070561309

[15] Hearon, K. - Nash, L. D. - Rodriguez, J. N. - Lonnecker, A. T. - Raymond, J. E. - Wilson, T. S. - Maitland, D. J. (2014): Recycling: a high-performance recycling solution for polystyrene achieved by the synthesis of renewable poly(thioether) networks derived from d-limonene *Advanced Materials,* Vol. 26, No. 10, pp. 1551–1551. https://doi.org/10.1002/adma.201470065

[16] Noguchi, T., Miyashita, M. - Inagaki, Y. - Watanabe, H. (1998): A new recycling system for expanded polystyrene using a natural solvent. Part 1. A new recycling technique. *Packaging Technology and Science*, Vol. 11, No. 1, pp. 19–27. https://doi.org/10.1002/(sici)1099-1522(199802)11:1<19::aid-pts414>3.0.co;2-5

[17] García, M. T. - Duque, G., Gracia, I. - de Lucas, A. - Rodríguez, J. F. (2009): Recycling extruded polystyrene by dissolution with suitable solvents. *Journal of Material Cycles and Waste Management*, Vol. 11, No. 1, pp. 2–5. https://doi.org/10.1007/s10163-008-0210-8

[18] Maharana, T. - Negi, Y. S. - Mohanty, B. (2007): Recycling of polystyrene. *Polymer-Plastics Technology and Engineering*, Vol. 46, No. 7, pp. 729–736. https://doi.org/10.1080/03602550701273963

[19] Yuan, Z., Chen, H., Tang, J., Chen, X., Zhao, D., & Wang, Z. (2007). Facile method to fabricate stable superhydrophobic polystyrene surface by adding ethanol. *Surface and Coatings Technology*, Vol. 201, No. 16-17, pp. 7138–7142. https://doi.org/10.1016/j.surfcoat.2007.01.021

[20] Gupta, T. K. - Kumar, S. (2018): Fabrication of carbon nanotube/polymer nanocomposites. *In Carbon Nanotube-reinforced Polymers*, pp. 61–81. https://doi.org/10.1016/b978-0-323-48221-9.00004-2

[21] Rouabah, F. - Dadache, D. - Haddaoui, N. (2012): Thermophysical and mechanical properties of polystyrene: influence of free quenching. *ISRN Polymer Science*, Vol. 2012, pp. 1–8. https://doi.org/10.5402/2012/161364

[22] Kim, S. C. (2010): Effect of molecular weight of polymer matrix on the dispersion of MWNTs in HDPE/MWNT and PC/MWNT composites. *Macromolecular Research*, Vol. 18, No. 5, pp. 512-518. https://doi.org/10.1007/s13233-010-0510-4

[23] Sun, J. (2007). D-limonene: safety and clinical applications. *Alternative Medicine Review*, Vol. 12, No. 3, pp. 259-264.

[24] Stalder, A. F. - Melchior, T. - Müller, M. - Sage, D. - Blu, T. - Unser, M. (2010): Low-bond axisymmetric drop shape analysis for surface tension and contact angle measurements of sessile drops. *Colloids and Surfaces A: Physicochemical and Engineering Aspects*, Vol. 364, No. 1-3, pp. 72–81. https://doi.org/10.1016/j.colsurfa.2010.04.040

[25] Yang, J. - Yu, K. - Zuo, Y. Y. (2017): Accuracy of axisymmetric drop shape analysis in determining surface and interfacial tensions. *Langmuir*, Vol. 33, No. 36, pp. 8914–8923. https://doi.org/10.1021/acs.langmuir.7b01778

[26] Thukkaram, M. - Sitaram, S. - Subbiahdoss, G. (2014). Antibacterial efficacy of iron-oxide nanoparticles against biofilms on different biomaterial Surfaces. *International JSournal of Biomaterials*, Vol. 2014, Article ID 716080, pp. 1-6. https://doi.org/10.1155/2014/716080

Ref.:
Regalado, Roderick Jesus Jude M. – **Punzalan**, Emmanuel A. – **Penaloza**, David P. Jr.: *One-pot preparation of PS/silica hydrophobic coating by solution-casting using D-limonene as dispersing medium*
Építőanyag – Journal of Silicate Based and Composite Materials, Vol. 71, No. 3 (2019), 80–83. p.
https://doi.org/10.14382/epitoanyag-jsbcm.2019.14

Sorption reseaches on the removal of the bond ammonia from the wastewater

Eleonora BUTENKO
PhD, assistant professor. She's learned of Donetsk National University (2002-2007). She has been working of Azov Sea State Technical University from 2007. Now she is Deputy Head of Department of Chemical Engineering and Technology of Azov Sea State Technical University. She is the author more than 70 scientific articles and two monographs.

Eleonora BUTENKO ▪ Azov Sea State Technical University, Mariupol, Ukraine ▪ butenkoeo@rambler.ru
Érkezett: 2018. 02. 14. ▪ Received: 14. 02. 2018. ▪ https://doi.org/10.14382/epitoanyag-jsbcm.2019.15

Abstract
Examined the formation of free and bound ammonia in various coking processes, the existing processes of capture and the impact of ammonia on the environment. Layered double hydroxide sorbents of different composition were obtained and investigated. The activity and selectivity of layered double hydroxides in the process of sorption of ammonia and its derivatives was investigated. It is shown that the main factor affecting the rate of the process is the strength of the basic sites. The efficiency of the use of sorbents for the removal of ammonia from the environment has been evaluated.
Keywords: ammonia water, coke oven production, anionic clays, sorption, kinetics, bound ammonia, free ammonia
Kulcsszavak: ammónia-víz, kokszolókemence, anionos agyagok, szorpció, kinetika, kötött ammónia, szabad ammónia

1. Introduction

Coke oven production deals with manufacturing of coal coke, coke oven gas, benzene, ethylene, different oils, resins etc. These products can be used as fuel or as raw materials for manufacturing of polymers, synthetic detergents, pesticides, nitrogen containing fertilizers and the like. The main task of coke oven production is coal treatment by means of the coking method. During such process operations like coal washing, coke quenching, gas purification from hydrogen sulphide and resin rectification water is contaminated mainly with volatile phenols, ammonia and resins [1-4]. It is also characterized by excessive concentrations of thiocyanates, sulphides, chlorides, presence of thiosulphides and values of PH, ranging from 7.1 to 8.

2. Analysis of the literature data and setting the objective of investigations

The bulk of ammonia at coal coking is formed by means of direct extraction of NH_3 at pyrolysis of nitrogen containing coal compounds. The amount of nitrogen, bound into ammonia reaches 11-15 % from its overall content. Ammonia recovery at coking of coals, extracted in the Donetsk basin is 0.25-0.30 %, while for Kuznetsk basin coals it could be up to 0.45 % per 1 ton of dry coal [5].

Ammonia is a gaseous substance, its density is 0.77 kg/m^3. It forms, when mixed with air an explosive mixture with explosiveness limits: 14 % the lower, 33% the higher (in volume); the temperature of ignition of ammonia is 780 °C [6]. Ammonia is a very toxic substance, it has a strong smell, tangible at its concentration in air 40 mg/m^3. Maximal permissible concentration of ammonia in the working area of industrial premises is 20 mg/m^3.

At low temperatures ammonia is well dissolved in water. *Table 1* shows solubility of ammonia in 100 ml of water [7].

Temperature [°C]	20	30	40	70	80	90
Solubility [g/100ml]	53.1	44.0	30.4	10.4	6.3	2.6

Table 1. Dependence of solubility of ammonia in water upon temperature, g/100ml
1. táblázat Az ammónia vízben való oldhatóságának hőmérséklet függősége, g/100ml

Ammonia is a valuable component of coke coals and it is economically beneficial to recover it from gas. It is a source for obtaining nitrogen fertilizer (ammonia sulphate) and it is the main reagent for extraction of pyridine bases in sulphate-pyridine department of recovery shop. Coke oven gas purification from ammonia is required due to the following reasons: at presence of oxygen, water vapours, hydrogen sulphide, and hydrogen cyanide in coke oven gas, ammonia exerts strong corroding action on the equipment and gas pipe-lines; it hampers recovery of benzol hydrocarbons from coke oven gas, as it causes rapid damage of stripping oil and violates the technological mode; when coke oven gas is used for domestic applications it forms poisonous nitrogen oxides in fire chambers. Ammonia removal from gas is an obligatory condition for normal functioning of coke oven production and it is strictly obligatory for application of coke oven gas for domestic use [8].

Ammonia removal from coke oven gas can be performed in two ways: 1) by absorption in cold water in apparatuses, that were named scrubbers, the method is based on good solubility of ammonia in water; 2) by absorption in sulphur acid in apparatuses of bubbling saturators (or absorbers), the method is based on reaction of ammonia neutralization by sulphur acid. The second method has found a wide application in industry [9].

In ammonia-tar liquor, formed at cooling of coke oven gas in cooling towers, gas collectors, or primary coolers the greater part of ammonia is in the form of various salts. Their presence in ammonia-tar liquor is explained by the fact that hydrogen sulphide, hydrogen chloride, hydrogen cyanide and other acid gases are consumed simultaneously with ammonia, the latter reacts with them, forming the corresponding salts.

Some of these salts-ammonium carbonate $(NH_4)_2CO_3$, ammonium sulphite $(NH_4)_2S$ and ammonium cyanide (NH_4CN) are so unstable, that they decompose when their water solutions are heated to the temperature, close to boiling temperature, emitting ammonia and the corresponding gases: H_2S, CO_2 and HCN. Ammonia, bound in the form of such salts is called volatile.

Ammonium chloride (NH_4Cl), ammonium thiocyanate (NH_4SCN), ammonium sulfate $(NH_4)_2SO_4$ belong to the group of stable compounds and they do not decompose at heating. Chemical methods of treatment are to be applied for recovery of ammonia from them. Ammonia, containing in ammonia-tar liquor in the form of these salt is called bound. It can be recovered by applying alkali, like slack lime (lime milk) stronger than ammonia on them.

Ammonia-tar liquor also contains some amount of phenols, pyridine bases, light oils, and naphthalene.

Ammonia, contained in ammonia-tar liquor in the volatile form is generally called total ammonia. Chemical composition of ammonia-tar liquor is characterized by presence of total ammonia, separate volatile ammonia, acids, bases and neutral admixtures.

Ammonia and ammonium salts content in ammonia-tar liquor is essentially determined by the cooling temperature of gas. The lower this temperature is the higher is the content of total ammonia in water. Moreover, the content of total ammonia in water depends on the specified gas cooling scheme: it is smaller when gas is cooled in tubular coolers and higher, when gas is cooled in direct action coolers. Ammonia-tar liquor of gas collectors salts, containing bound ammonia prevail.

Ammonia is the main and most valuable component of ammonia-tar liquor. It contains up to 0.1% ammonia from their resources per 1mt of dry charge. The amount of excessive ammonia-tar liquor to undergo recycling is usually 10-12 % from the coking charge. Utilization of these vast ammonia resources at large scale of coke oven production is a task of a paramount importance, as ammonia recovered there can be used for production of ammonia sulphate and recovery of pyridine compounds. *Table 2* shows an approximate composition of ammonia-tar liquor, supplied for treatment (at mixing of drainage from gas collectors and primary coolers), in g/l.

Modern process flow sheets of recycling of ammonia-tar liquor are closely connected with functioning of sulfate and pyridine departments and phenol-removing unit.

The process of distillation is used for recycling of ammonia-tar liquor, i.e. recovery of the solved ammonia from ammonia-tar liquor by means of live steam in distillation columns, equipped with bubble cup plates at 100-102 °C.

Total	7.0
Volatile	3.0
H_2S	1.3
CO_2	1.3
Phenols	1.5-2.0
Pyridine compounds	0.4-0.5

Table 2. Approximate composition of ammonia-tar liquor, g/l
2. táblázat Az ammónia-kátrány kompozit közelítő összetétele, g/l

Recycling of ammonia-tar liquor includes the following process operations: distillation of volatile ammonia from ammonia-tar liquor in evaporation column, phenol removal from water by means of live-steam method; decomposition of salts of bound ammonia inside the reactor by a solution of slack lime; distillation of bound ammonia in the column of bubble cup type [10].

The process of recovery of volatile ammonia from ammonia-tar liquor is based on a drastic reduction of solubility on water of ammonia, carbon dioxide, hydrogen sulphate, hydrogen cyanide, at water heating up to 98-100°C. At that decomposition of carbonates, sulphides, and cyanides takes place with recovery of ammonia and other gases, according to the following reactions:

$$(NH_4)_2CO_3 \rightarrow 2NH_3 + CO_2 + H_2O,$$
$$(NH_4)_2S \rightarrow 2NH_3 + H_2S,$$
$$NH_4CN \rightarrow NH_3 + HCN.$$

Ammonia-tar liquor of plants, where coals from the Donetsk basin are used has an increased content of bound ammonia salts (4 to 7 g/l).

However, the described methods do not permit to get fully rid of ammonia ions. Wastewaters contain sufficiently big amounts of ammonia ions. Water, drained into the Azov Sea, which is not completely recycled contaminates it and also underground waters.

3. The objective and tasks of investigations

The problem of removal of ammonia nitrogen from water is a vital one, as pollution of underground waters inevitably leads to pollution of fresh waters. Constant consumption of water, containing increased content of ammonia may cause chronic acidosis and changes in tissues. Moreover, there is a danger of uncontrolled nitrification resulting in formation of nitrites as an intermediate product, negative influence of which upon human organism is quite substantial. That is why purification of wastewaters from coke oven production is quite topical.

Various methods of additional purification, like, for instance, coagulation, bio-filtration, ionite purification, reverse osmosis, sorption methods with application of different sorbents are most commonly used. Economic and ecological components of these methods of additional purification differ very much.

Most promising and economically beneficial are sorption methods of additional purification with application of anionic clays of different compositions. Synthetic anionic clays possess high selectivity to ammonia ions, they are not costly, as they are waste products of chemical industry and there cannot be any problems with their utilization as at their thermal treatment the reverse process of desorption is not possible.

4. Experimental results

4.1. Recovery of double hydroxide sorbents

There are two principal methods of recovering main sorbents of hydroxide type: mechanical and chemical method and the method of precipitation from a liquid solution. Both these methods have advantages and drawbacks of their own.

By applying the method of displacement of oxides and salts with addition of water and also hydroxides and salts hydroxides, on the basis of zinc-chromium, calcium-aluminum,

copper-aluminum were received. The components in the corresponding, calculated quantities were placed into a glass and mixed with periodic addition of water for several hours, by means of a magnetic mixer. The biggest practical difficulty of this method is in the necessity of constant taking of samples to observe the progress of reaction, as it is impossible to determine the appearance of a new phase visually. That is why the bulk of catalysts was received by the method of basic precipitation.

By applying the method of precipitation various sorbents of hydroxide type were obtained and investigated $[Mg_2Al(OH)_6]OH$, $[Cu_2Al(OH)_6]OH$, $[Zn_2Cr(OH)_66]OH$, $[LiAl_2(OH)_6]OH$ et al. The main problem of the method of precipitation was formation of fine-disperse amorphous sediment of hydroxides, it making very difficult to filter it and flush it to remove alien ions. Increase of crystallinity was obtained by holding the sediment in mother waters at the temperature range 50-250 °C. In this case the sediment appeared to be more acceptable for work, but filtration took too much time. To speed up the process the mother waters were cooled, precipitated and then the sediment was separated by decanting. Then a new portion of flushing water was added, the solution was mixed again and settled. Unfortunately, it is not possible to reach a complete removal of alien cations, that is why these operations were alternated with filtration of the solution in vacuum. The process was repeated until the absence of qualitative reaction for cations in the flushing liquid. After recovery, basic double hydroxides were washed in KOH solution for deactivation of acid centres and transition of sorbents into basic state.

4.2 The methods of determination of ammonia content

The essence of the method is in determining of volatile ammonia by a direct titration with sulphur acid along the reaction. The way of determination: an aliquot part of ammonia water -10 ml is introduced into a conic bulb, then some distilled water is added, so that the sample's volume should be 100 ml and volatile ammonia is titrated by a solution of sulphur acid until orange methyl indicator acquires pink colour. Afterwards we add 5-7 drops of phenolphthalein indicator into this neutralized solution and 5 ml of 40 % solution of formaldehyde (formalin has to be preliminarily neutralized by NaOH solution in presence of phenolphthalein until appearance of pinkish colouring). In 2-3 minutes recovered acid is titrated by NaOH solution until appearance of pinkish coloring [11].

The error of the analysis with acid titrating, i.e. the difference between the evaluations should not exceed 0.02g/l.

4.3. Kinetic investigations

A sample of excessive water, containing ammonia in different compounds, 200 ml in quantity was loaded into a conic bulb, equipped with a contact thermometer and a reverse cooler, sorbents of various compositions were added and the mixture was mixed on a magnet mixer for a specified time span at certain temperature. Samples for analysis were taken at fixed intervals.

5. Results and discussion

The obtained sorbents were investigated for presence of basic sites of different strength (*Table 3*).

Sorbents	H_0, mol/l
$[Mg_2Al(OH)_6]OH$,	12.2
$[Zn_2Cr(OH)_66]OH$,	15.0
$[Mg_2Al(OH)_6]OH$, calcined at 650 °C	18.4
$[Zn_2Cr(OH)_66]OH$, calcined at 650 °C	45.0

Table 3. The basicity of sorbents
3. táblázat A szorbensek bázikussága

On the basis of the obtained data the values of activity of anionic sorbents were compared to the active sites of different strength. The quantity of added sorbent was 0.5 mol/mol from concentration of bound ammonia. The reaction flows very rapidly, that is why the temperature was decreased up to 5 °C to slow it down.

6. Conclusions

1. Removal of bound ammonia from excessive waters of coke oven production is possible with application of synthetic anionic clays of different composition.

2. Sorption capability of synthetic anionic clays is determined by concentration of active sites on their surface, the nature of the sites and their basicity.

3. Synthetic anionic clays, having strong active sites are the most efficient sorbents for precipitating ammonia ions.

References

[1] Butenko E. – Kapustin A. (2009): Adsorption treatment of contaminated water the modified adsorbents. *Ecology and industry*.Vol 3, pp. 45-48.

[2] Butenko E. – Kapustin A. (2009): Selective adsorption of anionic compounds of the main minerals of different composition. *The modern scientific bulletin*. – Belgorod. Vol 27 (53), pp. 105-110.

[3] Lurie Y.Y. – Rybnikova A.I. (1963): Chemical analysis of industrial wastewater

[4] Lazarev N.V. – Levina E.N. (1976): Harmful substances in industry. *Handbook for chemists, engineers and doctors*. Vol. 1. pp. 12-15.

[5] Butenko E. – Kapustin A. (2011): Pollution of the water basin in the industrial region of Mariupol. *Ecology and industry*. Vol 3, pp. 33-37.

[6] Zubitsky B.D. – Clerks S.N. – Chimari V.A. – Swede V.S. – Sychev S.S. – Nazarov V.G. – Ekgauz V.I. – Dementieva N.V. (2002): Industrial development of new treatment technology of coke oven gas to the destruction of ammonia. *Coke and Chemistry*. Vol. 5, pp. 27-31.

[7] Platonov O.I. – Egorov V.N. – Lutokhin N.N. – Melnikov I.I. – Chistyakov N.P. – Egorov M.A. – Krinitsyn E.N. – Shchukin R.I. (2005): Features of industrial technology for the catalytic decomposition of ammonia coke. *Coke and Chemistry*. Vol. 5, pp. 37-41.

[8] Zaretsky M.I. (2003): Isolation of nitrogenous bases of the fractions of coke production. *Coke and Chemistry*. Vol. 5, pp. 24 - 27.

[9] Koganovsky A.M. – Klimenko N.A. (1990): Adsorption of organic compounds from water.

[10] Karpin G.M. – Chizhov V.M. – Oskin I.S. (2006): The cost-effectiveness of the sulfuric acid method of cleaning coke oven gas from ammonia. *Coke and Chemistry*. Vol. 4, pp. 36.

[11] Grekova N.N. – Lebedev O.V. – Kapustin A.E. (1997): Problems indicator titration basic heterogeneous catalysts. *Ukrainian Chemical Journal*. Vol. 1, pp. 25-27.

Ref.:
Butenko, Eleonora: *Sorption reseaches on the removal of the bond ammonia from the wastewater*
Építőanyag – Journal of Silicate Based and Composite Materials, Vol. 71, No. 3 (2019), 84–86. p.
https://doi.org/10.14382/epitoanyag-jsbcm.2019.15

Fenntartható Cement- és Betonipari Technológiák V. című szakmai nap a Miskolci Egyetemen

2019. április 24.

Az elmúlt évek hagyományait követve idén is megrendezésre került a „Fenntartható Cement- és Betonipari Technológiák" c. szakmai nap. A rendezvénynek a Miskolci Egyetem Műszaki Földtudományi Kara adott otthont, 2019.április 24-én. A rendezvényen nyolc előadás került bemutatásra egyetemek és ipari cégek szakemberei által.

A világviszonylatban évente keletkező nagy mennyiségű ipari melléktermék és hulladék hasznosítása a megfelelő technológiák alkalmazásával, továbbfejlesztésével megoldható, továbbá környezetbarát anyagok fejlesztésére ad lehetőséget a CO_2 kibocsájtás és energiaigény csökkentése mellett, így megvalósítható a fenntartható nyersanyag-gazdálkodás. Mindemellett a hazai építőipar növekedése jelentős mennyiségű és jó minőségű nyersanyagot igényel a következő időszakban, amely további kihívásokat jelent a hazai ipar és K+F+I szektor számára. Erre épültek a szakmai nap előadásai is:

Dr. Farkas Géza ügyvezető igazgató, Perlit 92 Kft.
Perlit és trassz jelentősége az építőanyag iparban

Peity Ágnes területi képviselő, CRH Magyarország Kft.
Cement Magyarországon - másfél év értékesítés tükrében

Dr. George Nehma Salem egyetemi docens, *Dr. Nemes Rita* egyetemi docens, Budapesti Műszaki és Gazdaságtudományi Egyetem
A beton passzív védelme

P*aula Oliveira Figueired* MSc hallgató, *Dr. Carina Ulsen* egyetemi docens, *Dr. Maurício Bergerman* egyetemi docens, Sao Pauloi Egyetem, Brazília
Építési-bontási hulladékok hasznosítása Brazíliában – Recycling of Construction and Demolition Waste in Brazil

Szabó Roland tudományos segédmunkatárs, *Dolgos Fann* tanszéki mérnök, *Gulyás Benjámin* tanszéki mérnök, *Dr. Debreczeni Ákos* egyetemi docens, *Tóth Alfréd* tanszéki mérnök, *Dr. Mucsi Gábor* egyetemi docens, Miskolci Egyetem
Hulladékból üveghab és geopolimer hab alapú hőszigetelő anyag laboratóriumi és méretnagyítási kísérletei

Dr. Kristály Ferenc tudományos főmunkatárs, Miskolci Egyetem
Röntgen-pordiffrakció és Rietveld illesztés a nanokristályos és amorf kötőanyagok fejlesztésében

Papané Halyag Nóra tanszéki mérnök, *Dr. Kristály Ferenc* tudományos főmunkatárs, *Dr. Mucsi Gábor* egyetemi docens, Miskolci Egyetem
SEM EDX alkalmazása geopolimer fejlesztési kutatásokban

Dr. Rácz Ádám egyetemi docens, *Dr. Mucsi Gábor* egyetemi docens, Miskolci Egyetem
„Innovatív Finomőrlési-Szemcsetervezési Technológiák Laboratórium Fejlesztése A Miskolci Egyetem Fenntartható Természeti Erőforrás Gazdálkodás Kiválósági Központban" című GINOP 2.3.3. projekt eddigi eredményei

A tudományos előadásokat egy, a Miskolci Egyetemen nemrég indult projekt ismertetője követte, amely keretében beszerzett eszközök nagymértékben hozzájárulnak majd a szakterületen jelentkező K+F+I ipari igények kiszolgálására a többi kutatóműhellyel szorosan együttműködve. A tanácskozást egy laboratóriumi látogatás követte, amelyen a résztvevők megtekinthették a Műszaki Földtudományi Karhoz tartozó jól felszerelt laboratóriumokat.

A szakmai nap jó lehetőséget biztosított a területen működő cégek (cementgyárak, betonüzemek, minősítő szervezetek) és a kutatás – fejlesztés szakembereinek az eszmecserére, amelyre több mint 70 fő regisztrált.

A Szervezők bíznak a kutatóhelyek és ipari cégek által megkezdett együttműködések folytatásában mind a kutatás-fejlesztés-innováció, mind pedig a felsőfokú oktatás vonatkozásában, valamint a szakmai nap rendszeres megrendezésével hagyományt kívánnak teremteni.

A rendezvény szervezői: Szilikátipari Tudományos Egyesület, Cement Szakosztálya, Beton Szakosztálya, a MTA Földtudományok Osztály, Bányászati Tudományos Bizottság, Bányászati, Geotechnikai és Nyersanyagelőkészítési Albizottsága, az MTA MAB Nyersanyagelőkészítési és Környezeti Eljárástechnikai Munkabizottsága, valamint a Miskolci Egyetem, Műszaki Földtudományi Kar, Nyersanyagelőkészítési és Környezeti Eljárástechnikai Intézete, továbbá az Országos Magyar Bányászati és Kohászati Egyesület Miskolci Egyetemi Szakosztálya.

Study the effect of metformin in different pH of human blood medium using cyclic voltammetric technique

Muhammed Mizher RADHI ▪ Radiological Techniques Department, Health and Medical Technology College-Baghdad, Middle Technical University (MTU), Iraq ▪ mmradhi@yahoo.com

Moaayad Jassim AL-HAYANI ▪ Radiological Techniques Department, Health and Medical Technology College-Baghdad, Middle Technical University (MTU), Iraq

Mohamed Flayyh TAREEF ▪ Dean of Health and Medical Technology College-Baghdad, Middle Technical University (MTU), Iraq

Érkezett: 2019. 03. 24. ▪ Received: 24. 03. 2018. ▪ https://doi.org/10.14382/epitoanyag-jsbcm.2019.16

Abstract

Metformin HCl is a drug to treatment of different diseases such as ovary, diabetes, and slimming. Present study includes the electrochemical analysis by cyclic blood medium at different pH to evaluate the oxidation – reduction current peaks of the metformin compound which appeared at +750 and -750 mV respectively in acidic blood medium, while the oxidation current peak of the metformin was disappeared in alkaline blood medium with present of reduction one, so metformin acts as antioxidant reagent in alkaline blood medium. The study device the patients whom have taken metformin tablets as a treatment for diabetic disease must take ascorbic acid with metformin tablet to avoid the oxidation stress.

Keywords: metformin, blood, cyclic voltammetry, different pH, redox reaction
Kulcsszavak: metformin, vér, ciklikus voltametria, különböző pH, redox reakció

Muhammed Mizher RADHI
Professor, Department of Radiological Techniques, Health and Medical Technology College-Baghdad, Middle Technical University, Baghdad, Iraq. He received his PhD from University Putra of Malaysia (UPM) in 2010 in Electrochemistry, Nanotechnology. Research topics: conductivity of grafted polymer with nano-deposit and fabrication of sensors by nanomaterials to study drugs in blood medium by electrochemical analysis.

Moaayad Jassim AL-HAYANI
Assistant professor, currently he is a lecturer in the Department of Radiological Techniques, Health and Medical Technology College-Baghdad, Middle Technical University, Baghdad, Iraq. He received M.S.D. physiology (cardiovascular physiology), Baghdad University, College of Veterinary medicine 1988. His study focused on cardiovascular physiology.

Mohamed Flayyh TAREEF
Assistant Professor, Dean of the Health and Medical Technology College-Baghdad, Middle Technical University, Baghdad, Iraq. He received his PhD of Microbiology at Mustansiriah University, Baghdad, Iraq (2006). His study focused on microbiology (bacteriology).

1. Introduction

In the resent time scientists have chosen cyclic voltammetric technique to study medicines in blood medium [1-6].

Metformin HCl is known in chemical structure (1,1-dimethylbiguanide HCl) as shown in *Fig. 1*. In the pharmacy market it is traded under the name of Glucophage and it is used as a treatment of type 2 diabetes,[7,8] particularly for people who are overweight, has polycystic ovary syndrome, cardiovascular disease or cancer complications of diabetes [9,10].

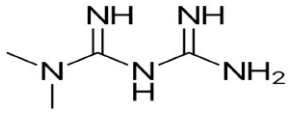

Fig. 1 Structure of metformin
1. ábra A metformin kémiai felépítése

A new method was used to determine metformin of pharmaceuticals, serum and urine from volunteers after spiking with metformin. The results were examined by a standard addition method. The number of pharmacological supplements and blood serum or urine matrix did not affect the determination of metformin [11]. The modified electrode, multi-walled carbon nanotubes (CNTs) composites on glassy carbon electrode (GCE) showed an excellent response to the oxidative current to determine metformin compound. In optimal conditions, a good linear peak current with concentrations in a range of 0.5 µm to 25 µm and a detection unit of 0.12 µm, as well as good repetition, was shown. The modified GCE with CNTs were applied successfully to determine metformin in pharmaceutical samples with good accuracy [12]. In 56 cases of lactic acidity strongly associated with metformin, the pH of blood lactate had no predictive value. One can reasonably rule out the accumulation of metformin as a prognostic factor. Ultimately, the determinants of metformin associated lactic acidosis were appeared to be the nature and number of influencing factors. Significantly, most patients survived - although the average pH is not consistent with a positive outcome under other conditions [13]. A newly developed spectral method was used in the present research project to determine the drug metformin hydrochloride, through the complication of copper (II). Color products were measured at 530 nm. The newly developed system for pharmaceutical analysis has been applied [14]. Metformin is an anti-diabetic drug that is widely used. HPLC is the most commonly used method for the analysis of metformin. Other methods include spectroscopy and potentiometric measurements. The drug is analyzed not only in a neat solution but also in pharmaceutical products alone and in combination with other drugs. Studies show that metformin can be successfully used to reduce the risk of cancer. However, a randomized trial is needed to see if the drug is useful among populations at risk for cancer. This review discusses the different methods used to analyze metformin and its potential role in carcinogen resistance [15].

In this work, metformin compound was studied by electrochemical analysis using cyclic voltammetric method in human blood medium at different pH.

2. Experimental methods

2.1 Cyclic voltammetric technique

EZstat (Potentiostat / Glvanostat) series from NuVant Systems (manufactured in the USA) was used to carry out the measurements. The electrochemical analysis cell was connected to the potentio-state and monitored by the program that was

installed on the computer to perform cyclic voltammetric measurement (CV). Silver / silver chloride (Ag / AgCl in 3 M KCl) as reference electrode and platinum wire (diameter 1 mm) was used as counter electrodes. The glass working carbon electrode (GCE) was used in this study after cleaning by polishing with alumina solution and treated using ultrasonic waterway for ten minutes for measurement performance.

3. Materials

Metformin HCl compound was received from Merk sante s.a.s (Germany). Blood samples from healthy humans obtained from the Baghdad Medical Center were collected for analysis after the serum was completely separated from the blood by an electronic centrifuge of type 8-1 (3,000 cycles / min). Deionized water was used to prepare water solutions. All serum blood samples were diluted with deionized water by 1: 9 ml (serum: deionized water), 10 ml of dilute serum was placed in a cyclic voltammetric cell.

4. Results and discussion

Previous research has addressed the effects of the use of metformin for the treatment of some diseases such as diabetes. In the current study we prove the effects of this treatment from an electrochemical study of the blood through the peaks of oxidation and reduction of metformin compound.

4.1 Effect alkaline pH on metformin in blood medium

According to the results of the pH studies of metformin in alkaline blood medium, *Fig. 2* illustrated the cyclic voltammogram of the oxidation – reduction current peaks of metformin in the range of alkaline pH (8-12), it was found the oxidation current peak was disappeared in this pH and the reduction current peak was enhanced in higher pH (12).

Also, the oxidation – reduction current peaks of metformin at neutral blood medium pH (7) has appeared at 0.750 and -0.5 V respectively and disappeared the oxidation one at alkaline blood medium (pH=12) as shown in *Fig. 3*. Thus, the metformin HCl compound act as anti-oxidative reagent in alkaline blood medium [16].

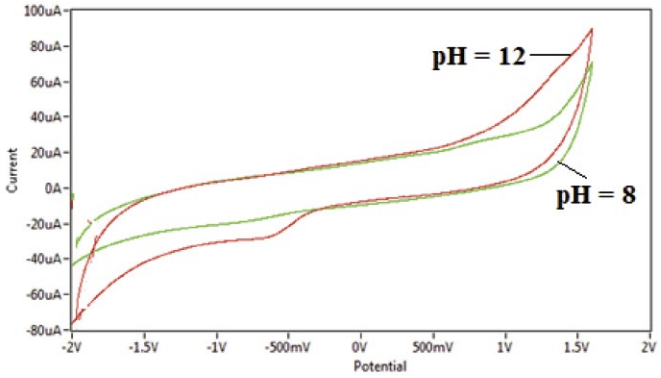

Fig. 2 Cyclic voltammogram of metformin in blood medium at different alkaline pH (8 and 12) using GCE and Ag/AgCl as working and reference electrode at scan rate 0.1 V sec^{-1}
2. ábra 8 és 12 pH-jú vérben lévő metformin ciklikus voltammogramja, GCE és Ag/AgCl használatával mint munka- és referenciaelektróda, 0,1 V sec^{-1}–es adatrögzítési sebesség mellett

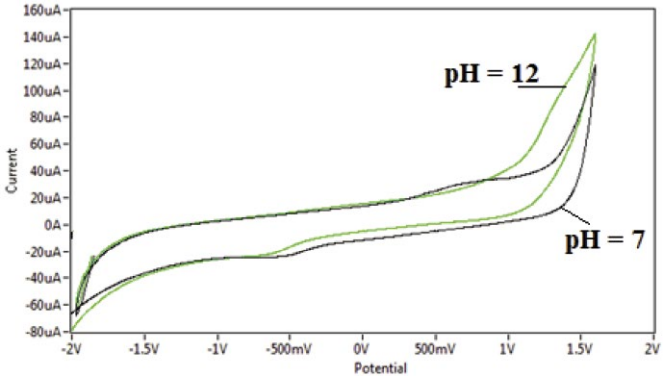

Fig. 3 Cyclic voltammogram of metformin in serum medium at different pH (7 and 12) using GCE and Ag/AgCl as working and reference electrode at scan rate 0.1 V sec^{-1}
3. ábra 7 és 12 pH-jú szérumban lévő metformin ciklikus voltammogramja, GCE és Ag/AgCl használatával mint munka- és referenciaelektróda, 0,1 V sec^{-1}–es adatrögzítési sebesség mellett

4.2 Effect acidic pH on metformin in blood medium

In the comparing study of metformin HCl compound between acidic and alkaline blood medium, it was found that oxidation – reduction current peaks of metformin have enhanced at acidic blood medium pH (3) as shown in *Fig. 4*, so the metformin in acidic blood medium acts as a catalyst for oxidation process [17].

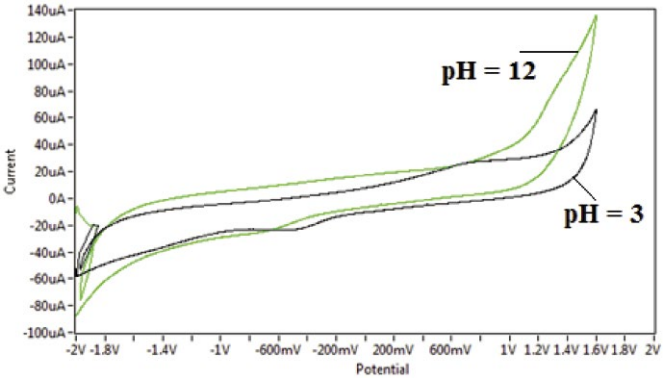

Fig. 4 Cyclic voltammogram of metformin in blood medium at different pH (3 and 12) using GCE and Ag/AgCl as working and reference electrode at scan rate 0.1 V sec^{-1}
4. ábra 3 és 12 pH-jú vérben lévő metformin ciklikus voltammogramja, GCE és Ag/AgCl használatával mint munka- és referenciaelektróda, 0,1 V sec^{-1}–es adatrögzítési sebesség mellett

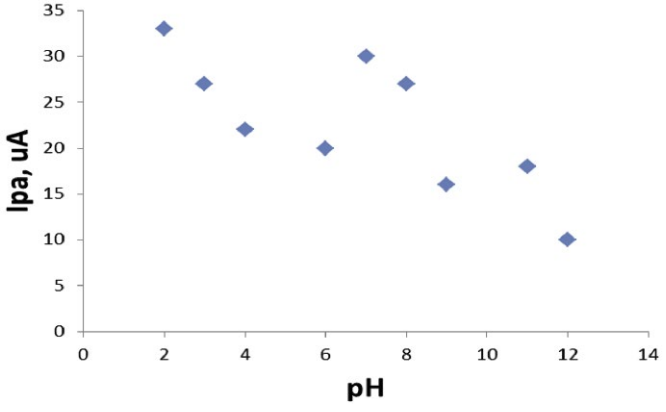

Fig. 5 Relationship between the oxidation current peak of metformin HCl and different pH of blood
5. ábra A metformin-HCl oxidációs csúcsa és a vér különböző pH-ja közötti kapcsolat

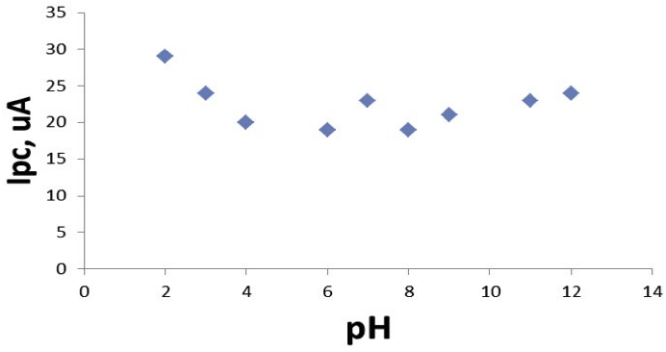

Fig. 6 Relationship between the reduction current peak of metformin HCl and different pH of blood
6. ábra A metformin-HCl redukciós csúcsa és a vér különböző pH-ja közötti kapcsolat

It was found from the results of the oxidation – reduction current peaks of metformine in different pH (2-12) that reduction current peak was enhanced in alkaline blood medium with disappearing the oxidation peak as shown in *Fig. 5* and *6*.

4.3 Effect of different medium on the redox current peaks of metformin

Fig. 7 illustrates the cyclic voltammogram of metformin HCl in each of blood and serum (plasma) at alkaline pH (12) to find the difference between the two electrolytes, which indicated that the blood and its serum have the same properties in electrochemical analysis and the overlapping of the cyclic voltammogram [18].

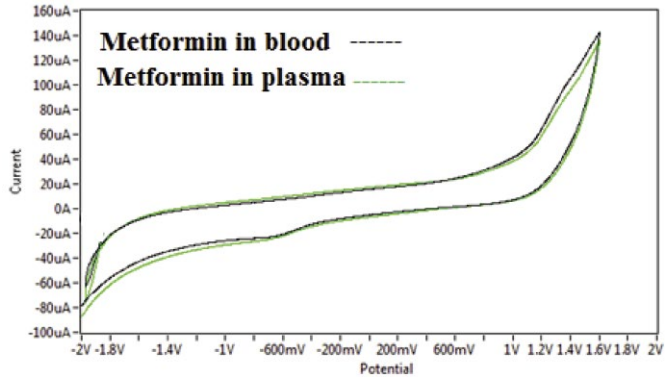

Fig. 7 Cyclic voltammogram of metformin in each of blood and plasma medium at alkaline pH (12) using GCE and Ag/AgCl as working and reference electrode at scan rate 0.1 V sec^{-1}
7. ábra 12 pH-jú vérben és plazmában lévő metformin ciklikus voltammogramja, GCE és Ag/AgCl használatával mint munka- és referenciaelektróda, 0,1 V sec^{-1}–es szkennelési sebesség mellett

5. Conclusions

Based on the present research, it can be concluded that the treatment of metformin HCl for all medical use cases need to be taken carefully as results from the electrochemical analysis of this compound in different pH of serum medium. It was found that using metformin in acidic blood medium causes an oxidative stress by enhancing the oxidation current peak which indicated as oxidative medicine, while the metformin acts as anti-oxidative drug in alkaline blood medium by disappearing the oxidation current peak. Thus, an important advice to the users of this medicine is to take the complements as blood alkaline synthesis such as ascorbic acid to make the treatment safer.

References

[1] Muhammed Mizher Radhi, Maysara Samer Khalaf, Zainab Oun Ali, Voltammetric study of saffron in blood mediated by modified glassy carbon electrode (GCE) with carbon nanotube (CNT/GCE), Journal of Silicate Based and Composite Materials, 2018, Vol. 70, No. 3, 78-81, https://doi.org//10.14382/epitoanyag-jsbcm.2019.1
[2] Muhammed Mizher Radhi, Lamyaa Abd Alrahman Jawad, Emad Abbas Jaffar Al-Mulla, Thamer Aboud Al-Dabbagh, Saffron in KCl Mediated by Glassy Carbon Electrode Using Cyclic Voltammetry, Nano Biomed. Eng., 2018, Vol. 10, Iss. 2, 181-185. https://doi.org/10.5101/nbe.v10i2.p181-185.
[3] Muhammed Mizher Radhi, Zuhair Numan Hamed, Selda Sabah Ezzaldeen, Emad Abbas Jaffar Al-Mulla, Effect of Micro- and Nanoparticles of Ampicillin Trihydrate on Blood Medium: A Voltammetric Study, Nano Biomed. Eng., 2017, Vol. 9, Iss. 3, 185-190. https://doi.org/10.5101/nbe.v9i3.p185-190
[4] Muhammed Mizher Radhi, Emad A. Jaffar Al-Mulla, Use of a grafted polymer electrode to study mercury ions by cyclic voltammetry, Res Chem Intermed, vol.41, no.6, 1413-1420, 2015.
[5] Muhammed Mizher Radhi, Hanaa Naji Abdullah, Majid Sakhi Jabir, Emad Abbas Jaffar Al-Mulla, Electrochemical Effect of Ascorbic Acid on Redox Current Peaks of CoCl2 in Blood Medium, Nano Biomed. Eng., 2017, Vol. 9, Iss. 2, 103-106. https://doi.org/10.5101/nbe.v9i2.p103-106.
[6] Muhammed Mizher R., Ali Abdulabbas Abdullah Albakry, Amani Mohammad Jassim, Sura Ali Alassady, Emad A. Jaffar Al-Mulla, Electrochemical Study of Pb(II) in Present of EachAscorbic Acid, Glucose, Urea and Uric Acid UsingBlood Medium as an Electrolyte, Nano Biomed Eng2016; 8(1): 9-15. https://doi.org/10.5101/nbe.v8i1.p9-15.
[7] Maruthur NM, Tseng E, Hutfless S, Wilson LM, Suarez-Cuervo C, Berger Z, Chu Y, Iyoha E, Segal JB, Bolen S. Diabetes Medications as Monotherapy or Metformin-Based Combination Therapy for Type 2 Diabetes: A Systematic Review and Meta-analysis. Annals of Internal Medicine., 2016, 164 (11): 740–51. https://doi.org/10.7326/M15-2650. Epub 2016 Apr 19
[8] Clinical Obesity (2nd ed.). Oxford: John Wiley & Sons. 2008. p. 262.
[9] Malek M, Aghili R, Emami Z, Khamseh ME, Risk of cancer in diabetes: the effect of metformin, ISRN Endocrinology. 2013: 636927. https://doi.org/10.1155/2013/636927. PMC 3800579. PMID 24224094.
[10] Type 2 diabetes and metformin. First choice for monotherapy: weak evidence of efficacy but well-known and acceptable adverse effects, Prescrire International. 23 (154): 269–72, 2014.
[11] Malik AlamgirMalik AlamgirAmir HayatAmir HayatAsghar Ali MajidanoAsghar Ali MajidanoMuhammad Yar KhuhawarMuhammad Yar Khuhawar, Spectrophotometric Determination of Metformin in Pharmaceutical Preparations, Serum and Urine using Benzoin as Derivatizing Reagent, J.Chem.Soc.Pak., Vol. 36, No. 2, 2014, 344.
[12] Mojtaba Hadi*, Haniyeh Poorgholi and Hossein Mostaanzadeh, Determination of Metformin at Metal–Organic Framework (Cu-BTC) Nanocrystals/Multi-walled Carbon Nanotubes Modified Glassy Carbon Electrode, S. Afr. J. Chem., 2016, 69, 132–139. https://doi.org/10.17159/0379-4350/2016/v69a16
[13] Kajbaf F, Lalau JD., The prognostic value of blood pH and lactate and metformin concentrations in severe metformin-associated lactic acidosis., BMC Pharmacol Toxicol. 2013, 12;14:22. https://doi.org/10.1186/2050-6511-14-22.
[14] Issam M. A. Shakir, Basim I. Al-abdli and Huda M. Nafea, Continuous Flow Injection Analysis (CFIA) of Metformin Hydrochloride using Microphotmeter Equipped with 530 and 550nm LED., Journal of Al-Nahrain University Vol.16 (4), December, 2013, pp.29-36 Science 29
[15] Wajiha Gul, Metformin: Methods of Analysis and Its Role in Lowering the Risk of Cancer, Journal of Bioequivalence & Bioavailability, Gul, J Bioequiv Availab, Volume 8(6): 254-259 (2016). https://doi.org/10.4172/jbb.1000305
[16] Ali K. Attia, Waheed M. Salem and Mona A. Mohamed Voltammetric Assay of Metformin Hydrochloride Using Pyrogallol Modified Carbon Paste Electrode, Acta Chim. Slov. 2015, 62, 588–594. https://doi.org/10.17344/acsi.2014.950

[17] Ambrish Singh, Eno. E. Ebenso, M. A. Quraishi, Theoretical and Electrochemical Studies of Metformin as Corrosion Inhibitor for Mild Steel in Hydrochloric Acid Solution, Int. J. Electrochem. Sci., 7 (2012) 4766 – 4779.

[18] M.KhanaJ.H.Kuipera Christine Sieniaws kab J.B.Richardson, Differences in concentration of metal debris in blood, serum, and plasma samples of patients with metal-on-metal hip resurfacing arthroplasty, Journal of Orthopaedics, Volume 13, Issue 4, 2016, Pages 450-454. https://doi.org/10.1016/j.jor.2015.10.006

Ref.:
Radhi, Muhammed Mizher – **Al-Hayani**, Moaayad Jassim – **Tareef**, Mohamed Flayyh: *Study the effect of metformin in different pH of human blood medium using cyclic voltammetric technique*
Építőanyag – Journal of Silicate Based and Composite Materials, Vol. 71, No. 3 (2019), 88–91. p.
https://doi.org/10.14382/epitoanyag-jsbcm.2019.16

Development of a laboratory scale continuous dry stirred media mill

Ádám RÁCZ:
Process engineer (Msc, 2008). He earned his PhD in 2014 in the field of grinding. He is currently associate professor at the Institute of Raw Materials Preparation and Environmental Processing, University of Miskolc. The main field of research and education is comminution and grinding.

László TAMÁS:
Process engineer (MSc, 2018, Bsc 2016). He finished his studies at the University of Miskolc, Faculty of Earth Science and Engineering, Institute of Raw Material Preparation and Environmental Processing.

Ádám RÁCZ ▪ University of Miskolc, Institute of Raw Material Preparation and Environmental Processing
László TAMÁS ▪ University of Miskolc, Institute of Raw Material Preparation and Environmental Processing

Érkezett: 2019. 04. 07. ▪ Received: 07. 04. 2019. ▪ https://doi.org/10.14382/epitoanyag-jsbcm.2019.17

Abstract
Stirred media mills are widely operated in the industry for the production of fine ground materials. The application of the mill type in dry mode came to the front in the recent years. Most of the operating dry mills have vertical orientation, however the horizontal type mills are also available on the market now, and some research is still ongoing for the development of this mill type. In the present study two development phase of a laboratory scale continuous dry, horizontal stirred media mill is presented. In the first phase the working principle of the mill, the air flow rate and feed rate were investigated. Later based on the operational experience and earlier results of the grinding experiments the mill has undergone significant changes resulted in a significant increase in the amount of air flow rate through the mill. The measurement results of the second phase led to that the mill has a significantly higher air flow rate and stable constant feed rate, however the control of the air flow during operation is essential to achieve the required product particle size.
Keywords: dry fine grinding, stirred media mill, continuous operation
Kulcsszavak: száraz finomőrlés, keverőmalom, folyamatos üzem

1. Introduction

Dry stirred media milling is a highly energy-efficient and promising technology that can be used to produce fine submicron ground materials, but there are still many problems to be solved in this area for wider industrial application. The operation of a horizontal dry stirred media mill was investigated by [1], found that increase of the stirrer speed produced finer material up to a point that further addition of energy was converted into heat causing decreased efficiency of the grinding operation, lower media fillings created inefficient grinding environments. Later in the same mill, the effects of chamber diameter and stirrer design on dry horizontal stirred mill performance was investigated [2], found that the larger gap between the stirrer edge and mill chamber performed more efficient grinding operation. Stirrer design tests were conducted with cross, wing and disc designs having the same diameter. At higher energy levels (>40 kWh/t) wing and cross design stirrers utilize more energy than the disc design to achieve the same degree of size reduction. Reduced milling performance of the wing and cross designs were attributed to increased mill chamber temperature which indicated that most of the energy was dissipated as heat. Dry grinding experiments in a self-modified horizontal stirred media mill was presented by [3]. It was revealed that dry fine grinding in continuously operated horizontal stirred media mills is strongly determined by both, machine related values like the choice of process parameters as well as product related characteristics like the powder flow ability. They confirmed the existence of optimum stressing conditions at comparatively low stressing energies. High powder flow abilities constantly lead to lower grinding efficiencies in the present study. However, also very low powder flow abilities are identified to decrease the grinding efficiency, as it causes unfavourable stressing conditions and an inefficient grinding media motion. The stirrer tip speed was identified to be a more critical process parameter than other values like bead size and bead material, since the deflector wheel is coupled with the stirrer shaft, the stirrer tip speed does not only influence the stressing energy of the beads, but also the retention behaviour of the wheel classifier.

In the present article, the first two development phases of a laboratory scale continuous dry horizontal stirred media milling system are presented.

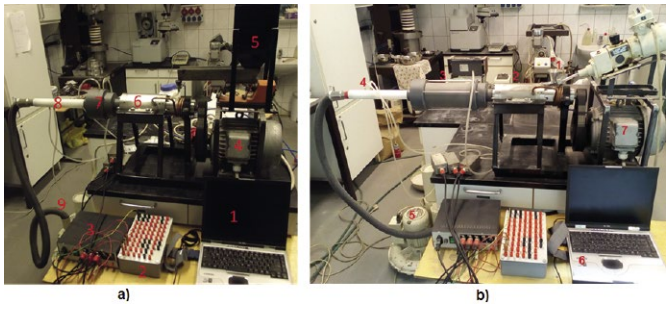

Fig. 1 *Continuous dry stirred media mill – first (a) and second (b) configuration*
1. ábra *Folyamatos üzemű száraz keverőmalom – az első (a) és második (b) konfiguráció*

2. Experimental

A continuous dry stirred media mill was developed and built, where the solid material is transported in the mill by air flow. The effective volume of the mill is 520 cm^3. The mill can be operated in open circuit mode. The stirred media mill is equipped with a six specially shaped triangle discs. The mill is double-walled to cool the grinding chamber. The operation of the motor and the ventilator is regulated by a frequency controller, so the rotor's revolutions per minute and circumferential speed could be adjusted. Parts of the milling system in the first configuration are as follows (*Fig 1a*): 1. Computer; 2. Electrical control board of the data acquisition

system; 3. Power supply of the data acquisition system; 4. Mill engine; 5. Silo and vibration feeder; 6. Stirred media mill; 7. Filter; 8. Venturi tube; 9. Ventilator.

The parts of the second configuration are as follows (*Fig 1b*): 1. Screw feeder; 2. Stirred media mill; 3. Filter; 4. Venturi tube; 5. Fan; 6. Data acquisition system; 7. Mill engine. Online measurement and data acquisition system was developed for the grinding system. For the data acquisition a self-written LabWindows program is used. The measuring system is capable to measure the static pressure after the mill (p1), the static pressure after the filter (p2) and the pressure drop in the Venturi tube (Δp). The velocity of the air in the Venturi tube is calculated from the pressure drop and therefore the volumetric flow rate of the air (Q) can be determined as well.

$$Q = A_2 \sqrt{\frac{2}{\rho} \cdot \frac{\Delta p}{1-\left(\frac{A_2}{A_1}\right)^2}} \qquad 1)$$

During the experiments limestone was used as model material for the grinding. The limestone powder was obtained from the Felnémet mine site. The limestone powder first was sieved at 106 μm by laboratory sieve and then the material was further separated in an air separator (type NETZSCH CFS 5 HD-S) to separate the most of the fine particles under 10 μm and to receive an appropriate feed for the grinding experiments. Rotor speed of the classifier was set to 3500 RPM, and the air flow rate was 63 m³/h.

The particle size distribution of the ground material was determined using a HORIBA LA-950V2 type laser particle size analyzer. From the measured data the computer calculated the particle size distribution according to the Mie-theory. During the measurement ultrasonic treatment was used for the dispersion of fine particles.

During the experiments with the first configuration 0.2, 0.4, 0.6 and 0.8 kg/h feed rate was applied. The effect of the rotor velocity was investigated at 6, 8, 10 and 11 m/s. To measure the effect of the air flow rate, the frequency of the ventilator rotor was moderated between 20 and 35 Hz.

During the grinding experiments of the second configuration 0.8-1 and 1-1.2 mm zirconium silicate grinding media were used. The feed rate was constant during all grinding experiments 0.6 kg/h. Grinding media filling ratio was set to 0.6. The exact air flow rates were measured during the experiments.

3. Results

The operation of the mill configuration "A" was investigated in several steps. First the fan operation was tested. It was found that the air flow through the mill increasing linearly by the frequency of the fan current in case of empty mill. Later the mill was filled with grinding media and the mill rotor at different velocities was operated (*Fig. 2*). The air flow rate was not affected by the rotor circumferential velocity, at a certain fan current frequency. After evaluating the pressure loss data, it became clear that the highest pressure loss is on the filter.

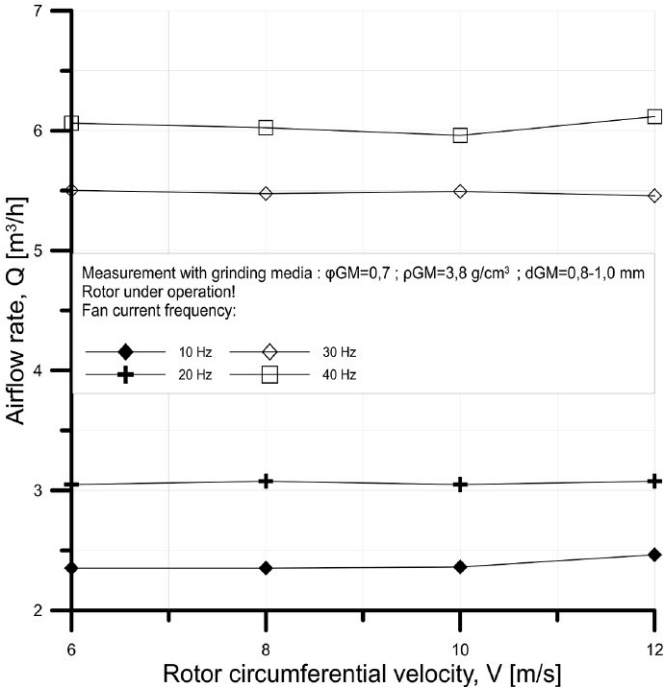

Fig. 2 Airflow rate at different rotor circumferential velocities
2. ábra Légáramok különböző rotor kerületi sebességek mellett

During the milling experiments with the configuration A it could be observed that the airflow rate decreases as a function of the grinding time (*Fig 3*). During grinding the pressure loss on the filter increases with the material layer on the filter surface increases. As a result, the average internal air velocity in the grinding chamber decreases, and thus the amount of the transported material inside the mill decreases, which could lead to a blockage in the mill. To solve this problem, at longer grinding experiments the filter should have been cleared, and thus the pressure loss decreased, and the mill was able to operate stable again.

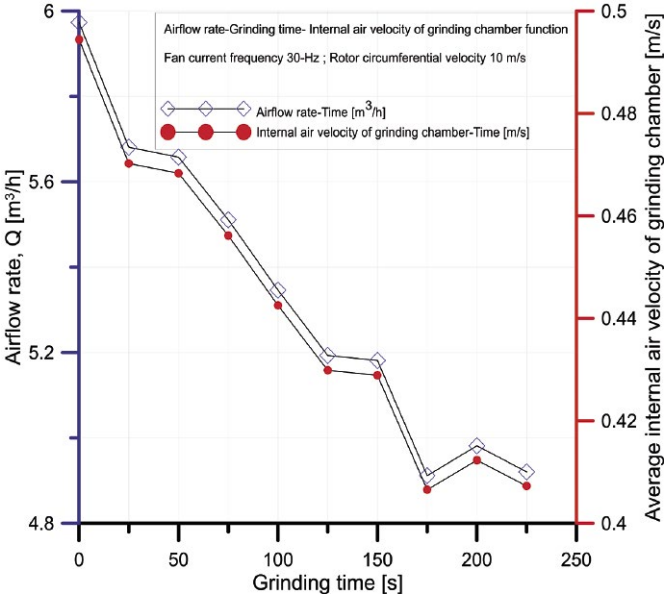

Fig. 3 Airflow rate and air velocity changes within the mill during grinding
3. ábra Légáram és légsebesség változás a malmon belül őrlés közben

After the first grinding experiments systematic grinding experiments were carried out with the construction A at different airflow and feed rates. The effect of the feed rate on the cumulative undersize of the product can be seen in *Fig 4*. In the feed material less than 3% are under 10 μm. After grinding at different feed rates the ratio of the fine (<10um) particle significantly grows up to 30%. The finest product was achieved by the 0.2 kg/h feed rate. Higher feed rates resulted in coarser product. From the cumulative undersize curves it can be seen that the maximal particle size of the feed did not decrease, so the stress energy inside the mill was not enough to the effective body breakage of the particles.

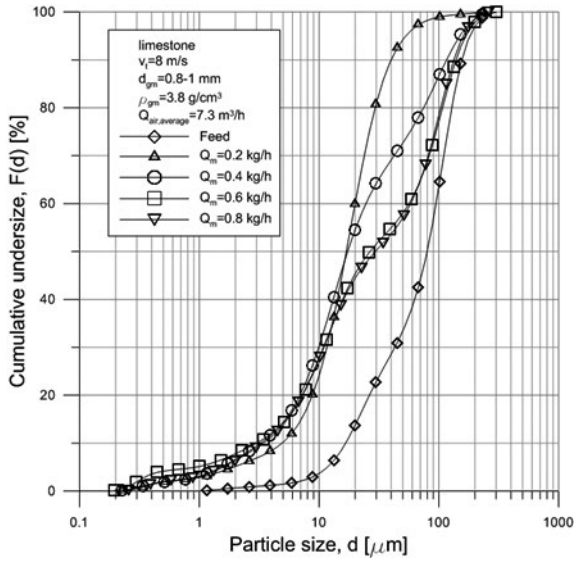

Fig. 4. Effect of the feed rate on the cumulative undersize of the product
4. ábra A feladási tömegáram hatása az őrlemény szemcseméret-eloszlására

The effect of the feed rate on the median particle size at different air flow rates can be seen in *Fig 5*. At a certain air flow rate, the higher the feed rate, the higher the median particle size. At a certain feed rate the higher the air flow rate, the finer the product. The lowest median particle size was achieved at 0.2 kg/h feed rate and 7.3 m³/h average air flow rate, its value was 16.8 μm. At low feed rates (low mill loading) increasing the air flow rate did not have significant effect on the median particle size, the grinding is sufficient, the ground material is fine. Increasing the feed rate, at same air flow rates, the product became coarser, because the residence time in these cases was determined by the quantity of feed rate. However, at the same feed rate, the higher air flow gives a finer product. The explanation for this is that the grinding efficiency was improved by increasing the air flow. The main limiting factor in the production of fine materials by dry grinding is the adhesion of the fine particles and the sticking of the particles on the mill liners and on the grinding beads, which decreases the efficiency of grinding. The higher air flow reduced these effects more sufficiently, so the product became finer [4].

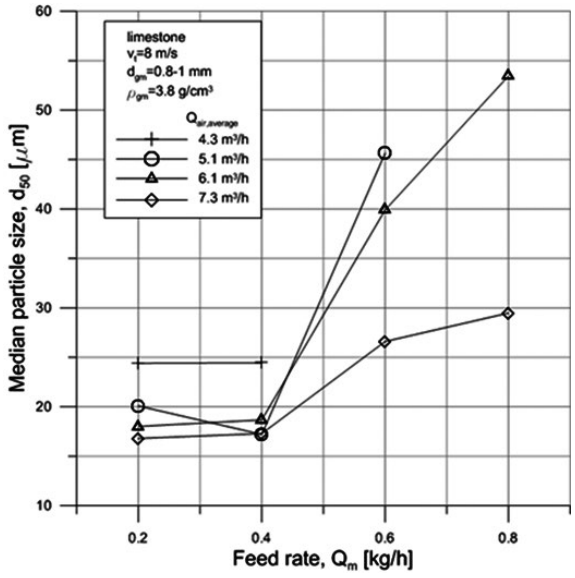

Fig. 5 Effect of the feed rate on the median particle size at different air flow rates
5. ábra A feladási tömegáram hatása a median szemcseméretre különböző légáramok esetén

Based on the grinding results and the operational experiments problems of the first configuration came to the surface:

- Feeding of fine material couldn't be done, because of the feeding tubes' blockage, the continuous and constant feeding of the mill also was a problem because the air flow rate influenced the feed mass flow.
- The applied filter wasn't efficient enough, after a short period of time it had to be cleaned.
- The pressure drop of the mill and filter was too high, thus the energy consumption of ventilator was high.

From the grinding experiments with configuration A it can be stated that at the applied air flow rates the material transported not only by air, but by a simple flow through as well.

Based on the earlier grinding experiments and results the continuous dry stirred media milling system was undergone improvements that enable more efficient grinding and more reliable operation. For this reason, first of all, the feeding technique had to be changed, which in practice was realized in the form of a storage unit with a larger cone angle and a screw feeder placed beneath it. In addition to providing continuous and stable mass flow, it appears as a further advantage to completely separate the material feed and airflow. In this way, the material feed and the airflow rate became independent. To reduce the pressure loss on the filter, it was further changed to a bag type. The pressure loss of the mill was also decreased. Measurements made with the "B" mill construction, similarly to previous results, were carried out systematically, with pre-planned steps, helping to improve the comparability of the data obtained from the measurements of the two different constructions. During the first measurement experiment, the operation of the newly built air filter system was tested, relying on data from the previous measurement results, with a feed rate of 0.6 kg/h. In the grinding experiments the mill was operated for 40 minutes and sampling and filter cleaning was carried

out after every 10 minutes. The change of the air flow rate of such grinding experiment can be seen in *Fig 6*. After each filter cleaning the starting air flow rate decreased. The level of the air flow rate however became significantly higher than in the case of construction A, so the pressure loss of the mill and filter was successfully decreased. The air flow rate linearly decreases as a function of the grinding time. The starting 26 m^3/h air flow rate was decreased to 20 m^3/h after 40 minutes operation.

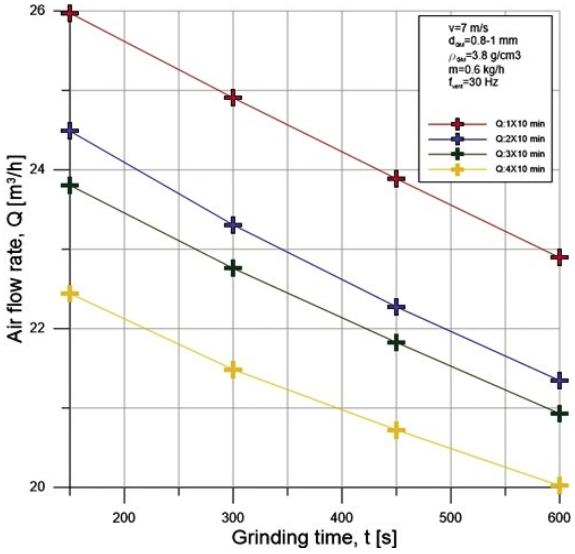

Fig. 6 Effect of operational time on the air flow rate
6. ábra Az üzemelési idő hatása a légáramra

The cumulative undersize of the ground material at 7 m/s rotor velocity and after 40 min operation can be seen in *Fig. 7*. The product of the mill is finer than the feed, however the degree of the size reduction is relatively low. The significantly higher air flow rates decreased the residence time of the particles inside the mill, thus the stress number of the particles, so the grinding was not sufficient.

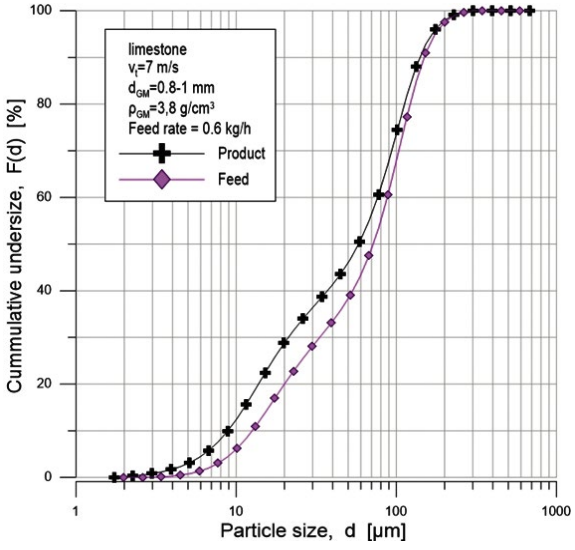

Fig. 7 Cumulative undersize of the product after grinding at 7 m/s rotor velocity
7. ábra Az őrlemény szemcseméret-eloszlása 7 m/s rotor kerületi sebesség esetén

Increasing the stress energy by increasing the grinding media diameter to 1-1.2 mm and the rotor circumferential velocity to 10 m/s did not resulted in finer product (*Fig. 8*). This can be explained by the centrifugal forces created by the higher rotor velocity. Possible way to increase the grinding efficiency is to significantly increase the size of the grinding beads and reduce the rotor velocity significantly. The larger grinding media results in lower pressure loss in the mill and higher pore volume which can help the transportation of the ground material inside the mill.

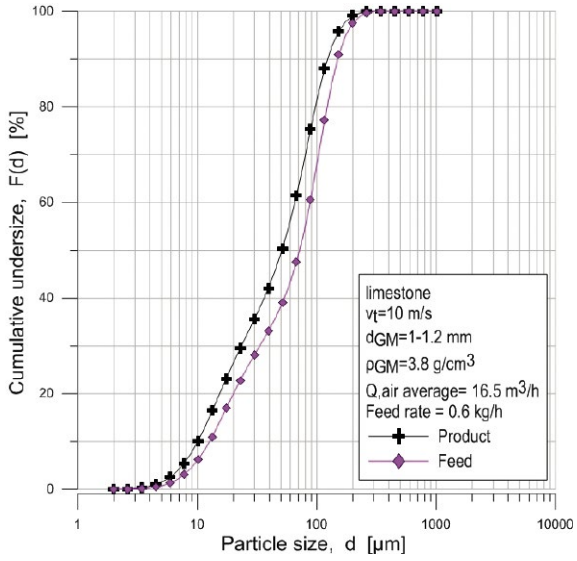

Fig. 8 Cumulative undersize of the product after grinding at 10 m/s rotor velocity
8. ábra Az őrlemény szemcseméret-eloszlása 10 m/s rotor kerületi sebesség esetén

The effect of the air flow rate on the product fineness can be seen in *Fig. 9*. The higher ventilator current frequency resulted in higher average air flow rates. The higher the air flow rate, the finer the product. Higher air flow rate results in lower residence time in the mill; however the higher air flow rate helps to discharge the particles from the mill.

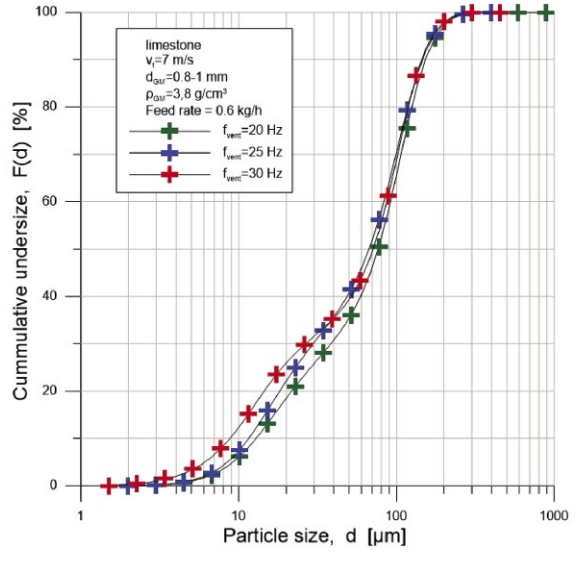

Fig. 9 Cumulative undersize curves of the ground material at different air flow rates
9. ábra Az őrlemények szemcseméret-eloszlása különböző légáramok esetén

This can be seen in *Table 1*, where the ratios of the product mass at different air flow rates are presented. The higher air

flow rate is more effective to discharge the fine particle from the grinding chamber. At lower air flow rate possibly more fine particle was created because of the longer residence time, but with the lower air flow the product particle was not discharged from the mill sufficiently, so more and more fine particle remained in the grinding chamber, which could result the blockage of the mill at longer operational time.

Average air flow rate [m³/h]	Ratio of the product mass [%]
24.2	86.3
19.5	83.4
16.8	79.3

Table 1 Ratio of the product mass at different air flow rates
1. táblázat A termék tömegének aránya különböző légáramok esetén

4. Conclusions

In the present study the first two development phase of a laboratory scale horizontal dry stirred media mill was presented. During the development the stable operational time of the mill was successfully extended, however further improvements are necessary for a long term operation of the milling system. The results proved that the mill can effectively produce particles below 10 microns, however the control of the product particle size requires constant air flow rate during grinding. To ensure this, the future goal is to build a controlling system for the fan, which can compensate the increase in pressure loss of the mill and filter during grinding.

5. Acknowledgement

The research work described in this article was supported by the European Union, as part of the project EFOP-3.6.1-16-2016-00011 "Youthful and Renewable University - Innovative Knowledge City - the Institutional Development of the University of Miskolc for Intelligent Specialization". Co-financed by the European Social Fund. The research work was supported by the János Bolyai Research Scholarship of the Hungarian Academy of Sciences.

References

[1] O. Altun, H. Benzer, U. Enderle, Effects of operating parameters on the efficiency of dry stirred milling, Miner. Eng. 43–44 (2013) 58–66. https://doi.org/10.1016/j.mineng.2012.08.003.
[2] O. Altun, H. Benzer, U. Enderle, The effects of chamber diameter and stirrer design on dry horizontal stirred mill performance, Miner. Eng. 69 (2014) 24–28. https://doi.org/10.1016/j.mineng.2014.07.008.
[3] P. Prziwara, S. Breitung-Faes, A. Kwade, Impact of the powder flow behavior on continuous fine grinding in dry operated stirred media mills, Miner. Eng. 128 (2018) 215–223. https://doi.org/10.1016/j.mineng.2018.08.032.
[4] Á. Rácz, L. Tamás, I. Gombkötő, B. Csőke, J. Faitli, Effect of the milling parameters on the product dispersity and energy consumption in a continuous dry air- transported stirred media mill, Proc. 15th Eur. Symp. Comminution Classif. (2017) 1–5.

Ref.:
Rácz, Ádám – **Tamás**, László: *Development of a laboratory scale continuous dry stirred media mill*
Építőanyag – Journal of Silicate Based and Composite Materials, Vol. 71, No. 3 (2019), 92–96. p.
https://doi.org/10.14382/epitoanyag-jsbcm.2019.17

CALL FOR PAPERS

ICCM 2019
Aug 06-07, 2019
Amsterdam, The Netherlands

The International Research Conference is a federated organization dedicated to bringing together a significant number of diverse scholarly events for presentation within the conference program. Events will run over a span of time during the conference depending on the number and length of the presentations.

ICCM 2019 : International Conference on Composite Materials is the premier interdisciplinary forum for the presentation of new advances and research results in the fields of Composite Materials. The conference will bring together leading academic scientists, researchers and scholars in the domain of interest from around the world. Topics of interest for submission include, but are not limited to:

Additive manufacturing
Applications
Bio-based composites
Biomimetic composites
Ceramic matrix composites
Concrete and cementitious composites
Damage and fracture
Durability and ageing
Experimental techniques
Fibers and matrices
FRP reinforced concrete
Health monitoring
Hybrid composites
Infrastructure
Interfaces and interphases
Interlaminar reinforcements
Joint and bearing behaviour
Life cycle analysis and sustainability
Low cost technologies
Mechanical and physical properties
Metal matrix composites
Multifunctional composites
Multiscale modelling
Nanocomposites
Nanotechnologies
NDE technologies

https://waset.org/conference/2019/08/amsterdam/ICCM

Preparation and synthesis of hydroxyapatite bio-ceramic from bovine bone by thermal heat treatment

Hassanen L. JABER
a PhD student in the Doctoral School on Materials Sciences and Technologies at Óbuda University, Hungary and Lecturer at the Biomedical Engineering Department, Faculty of Engineering, University of Thi-Qar, Nasiriyah, Iraq. His research activities focus on Additive manufacturing, Ti alloys, and Hydroxyapatite.

Tünde Anna KOVÁCS
associate professor in the Óbuda University, Donát Bánki Faculty of Mechanical and Safety Engineering, Materials Technology Department, Her interest focus material science, composites and metal alloys testing, manufacturing and innovations.

Hassanen L. JABER ▪ Doctoral School on Materials Sciences and Technologies, Óbuda University, Budapest, Hungary ▪ Biomedical Engineering Department, Faculty of Engineering, University of Thi-Qar, Nasiriyah, Iraq ▪ hassen.jaber@bgk.uni-obuda.hu

Tünde Anna KOVÁCS ▪ Donát Bánki Faculty of Mechanical and Safety Engineering, Óbuda University, Budapest, Hungary ▪ kovacs.tunde@bgk.uni-obuda.hu

Érkezett: 2019. 04. 07. ▪ Received: 07. 04. 2019. ▪ https://doi.org/10.14382/epitoanyag-jsbcm.2019.18

Abstract

Calcium phosphate, particularly hydroxyapatite (HAp) is an important material in biomedical engineering applications. The development of HAp is continued rising due to the similarity and biomimetic requirements to the hard tissue of human body such as bone and dental. The purpose of our work was to produce and describe HAp bioceramic powder from environmental and cheap source (Bovine bone) by thermal process at various calcination temperatures. The analysis of Fourier transform infrared spectroscopy (FTIR) verified the formation of HAp because of the existence peaks related to phosphate and hydroxyl groups. The analysis of Raman confirmed findings of the FTIR the formation of HAp due to the appearance of peaks at 960 and 920 cm^{-1} related to a phosphate group. A result of Energy-dispersive X-ray spectrometry (EDS) also referred to Ca/P atomic ratio at 1000 °C was 1.6 that has been near stoichiometric hydroxyapatite (1.67) in human body.

Keywords: Calcium phosphate, Calcination process, Hydroxyapatite, Tricalcium phosphate
Kulcsszavak: kálcium foszfát, meszesítési folyamat, hidroxiapatit, trikalcium foszfát

1. Introduction

Calcium phosphate (CaP) ceramics are a group of ceramic materials including calcium ions (Ca^{2+}), different phosphate ions [PO_4^{3-}, PO_4, $P_2O_7^{4-}$], and sometimes hydroxide (OH^-) or carbonate (CO_3^{2-}) ions [1]. CaP can be divided into 3 kinds: Hydroxyapatite (HAp), Tricalcium phosphate (TCP), and Tetracalcium phosphate (TTCP) based on atomic ratio of Ca/P [2]. It is common knowledge that atomic ratio of Ca/P is the main factor in identifying the bioactivity and dissolution property of CaP. A decrease in Ca/P atomic ratio will increase the disintegration rate of CaP [3]. Atomic ratio of Ca/P in bone and dental of human body exceeds (1.67) represents HAp [$Ca_{10}(PO_4)_6(OH)_2$] in comparison with Ca/P atomic ratio of TCP (1.5) and TTCP (2) [4].

Due to the continued rising similarity and biomimetic requirements to the hard tissue of human body such as bone and dental, the use of HAp in biomedical and dental applications is rapidly increasing. In addition, the need for biocompatibility, osteoconductivity, and bioactivity in the biomedical application, tooth implants, and maxillofacial surgery, make this ceramic valuable for applications in the medical engineering.

HAp is the one of the major constituent of hard tissue (bone and teeth) of human body. *Table 1* shows biological, mechanical, and physiochemical, properties of HAp [5]. HAp can be produced in two methods including chemical methods [6][7] and natural resources[8][9]. HAp typically synthesized from the chemical methods presents some drawbacks: they are having cytotoxicity [10], hazardous chemicals [11] and relatively high cost [4]. On the other hand, HAp synthesized from the natural resources that can be used without any drawbacks in terms of similar chemical composition and physical properties [12].

Properties	Data	Properties	Data
Chemical composition	$Ca_{10}(PO_4)_6(OH)_2$ or $Ca_5(PO_4)_3(OH)$	Hardness (HV)	600
Ca/P molar ratio	1.67	Decomposition Temp. (°C)	More than 1000
Crystal system	Hexagonal	Melting point (°C)	1614
a=b **c**	0.942 nm 0.688 nm	Thermal conductivity (W/cm. K)	0.013
Young's modulus (GPa)	80-110	Biocompatibility	High
Elastic modulus (GPa)	114	Bioactivity	High
Density (g/cm³)	3.16	Biodegradation	Low

Table 1 Physiochemical, mechanical and biological properties of HAp [5][13][14]
1. táblázat A HAp. Fizikokémiai, mechanikai és biológiai tulajdonságai

The purpose of our work was to produce and describe HAp bioceramic from environmental and cheap source (Bovine bone) by thermal process at various calcination temperatures. This study is divided into four steps.

- Calcine of the Bovine bone at different temperatures (600-1000) °C for 2 hours.
- Calculate the Ca/P atomic ratio of calcined bones at different calcination temperatures by using energy-dispersive X-ray spectrometry (EDS).

- Determine the best atomic ratio of Ca/P that is close to 1.67 and that represents HAp.
- Characterize the HAp by different techniques such as Fourier transform infrared spectroscopy (FTIR), Raman spectrum, Scanning electron microscopy (SEM), and atomic force microscopy (AFM).

2. Experimental procedure

2.1 Bovine bone preparation

Bovine bone femur was provided by a local meat shop and cut into small pieces. The bone pieces were boiled in water for 2 h and washed utilizing a strong water jet to take out the adhering meat. Drying process was taken at 50 °C for 1 h in a furnace and afterward dried at room temperature for 2 weeks. Finally, the bovine bones were submerged in acetone for 30 min and cleaned with water for several times. *Fig. 1* shows the bovine bone after preparation with yellowish white color.

Figure 1 Bovine bone after preparation
1. ábra Szarvasmarha csont előkészítés

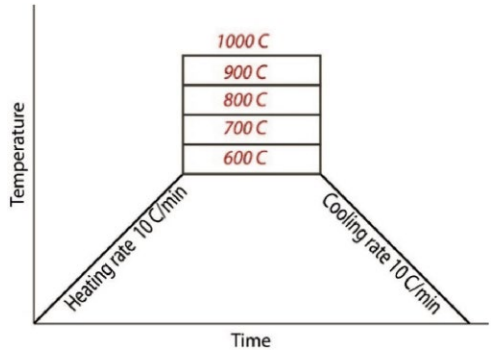

Fig. 2 Calcination process schedule
2. ábra Meszesítési folyamat leírás

Fig. 3 Bovine bone after calcination process
3. ábra Szarvasmarha csont meszesítési eljárás után

2.2 Calcination process

The bovine bones were calcined in a muffle furnace at various temperatures for 2 h. Calcination temperature was incrementally increased from 600 to 1000 °C with a step size of 100 °C. *Fig. 2* shows the calcination process schedule. The heating and cooling rate were kept constant at 10 °C min^{-1}. *Fig. 3* shows the color of bovine bone after calcination changes from yellowish white to white.

2.3 Characterization of calcined bone

Energy-dispersive X-ray spectrometry (EDS) was used to analyze localized chemical composition of calcined bone and determined the atomic ratio of Ca/P. Fourier transform infrared spectroscopy (FTIR) spectra were utilized so as to achieve the functional groups in calcined bone in the scope of 400 – 4000 cm^{-1}. The crystalline phases of the sample were determined by utilizing Raman spectroscopy. scanning electron microscopy (SEM) and Atomic force microscopy (AFM) were carried out to capture the surface morphology and topography of the calcined bone powder.

3.Results and discussion

3.1 Energy-dispersive X-ray spectrometry (EDS)

Table 2 shows EDS analysis of calcined bone at various temperatures. As can be seen, increasing calcination temperature from 600 to 1000 °C lead to the decreasing of Ca/P atomic ratio from 2.425 to 1.6. It was decided that the best calcination temperature for this study was 1000 °C due to Ca/P atomic ratio at this temperature was 1.6 that has been near stoichiometric hydroxyapatite (1.67) in human body. The result of EDS also referred to the presence of primary constituents such as Ca and P with some minor constituents such as Mg, Na, Cl, K, Si, and O. Piccirillo et al. [15] in their work on the characterization of HAp and TCP mentioned that these minor components such as Na and Cl improves on biocompatible and osteointegration.

temperature / Elements wt%	600 °C	700 °C	800 °C	900 °C	1000 °C
C	2.878	2.373	2.628	2.567	3.050
O	29.474	35.277	34.945	37.080	42.348
Na	0.539	0.785	1.042	1.154	1.508
Mg	0.398	0.526	0.564	0.554	0.734
Si	1.644	1.959	2.146	1.360	1.012
P	15.424	16.042	16.114	16.557	17.095
Cl	0.248	0.101	0.103	0.087	0.095
K	0.997	0.864	0.952	0.671	0.442
Ca	48.398	42.073	41.507	39.972	33.716
Ca/P ratio	2.425	2.026	1.990	1.865	1.6

Table 2 Chemical composition (wt%) of calcined bovine bone at various temperatures
2. táblázat Különböző hőmérsékleten meszesített szarvasmarha csontok kémiai összetétele (tömeg %)

3.2 FTIR and Raman of calcined bone at 1000 °C

Fig. 4 shows a FTIR spectra of calcined bone at 1000 °C. A typical HAp molecules structure is indicated by the presence of peaks matching to phosphate and hydroxyl groups. The

organization of HAp structure is dependent on this kind of groups [16]. Phosphate groups are a common part of FTIR spectra of HAp, which can be divided into three vibrational modes: symmetric stretch, asymmetric stretch and bending. The symmetric stretch mode is represented in FTIR spectra (*Fig. 4*) at the peak 960 cm^{-1} corresponding to PO_4^{3-}, asymmetric stretch mode is represented at the peaks 1090-600-568-460 cm^{-1} corresponding to PO_4, and bending mode is represented at 1025 cm^{-1} corresponding to PO_4^{3-}. The peak at 630 cm^{-1} is represented due to the vibrational of the hydroxyl group. In addition, the presence of 850 cm^{-1} band in spectra corresponding to P-OH related to HPO_4 group. A remarkable feature of HAp is the presence of HPO_4 group. The phosphate and hydroxyl groups were corresponded in accordance with [16][13][17].

The other test carried out with Raman spectrum (*Fig. 5*) confirmed findings of the FTIR the formation of HAp due to the appearance of peaks at 960 and 920 cm^{-1} related to a phosphate group [18].

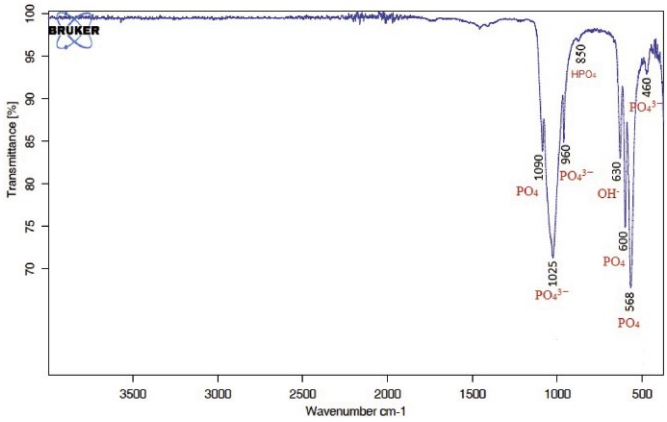

Fig. 4 FTIR spectra for calcined bone powder at 1000 °C calcination temperature
4. ábra 1000 °C-on meszesített porított csont FT-IR spektroszkópia

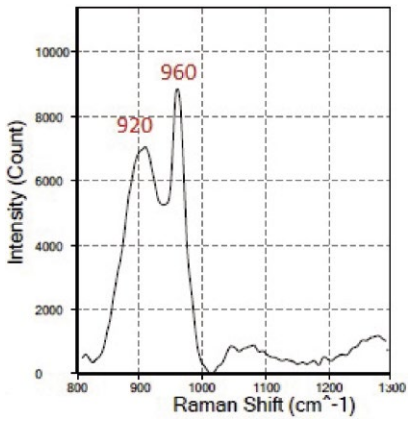

Fig. 5 Raman spectrum of Bovine bone heated at 1000 °C
5. ábra 1000 °C-on hevített szarvasmarha csont Raman spectroszkopia

3.3 SEM and AFM of calcined bone at 1000 °C

The result of SEM is presented in *Fig. 6* with different magnifications. The shape of HAp particles was irregular like needle and polygonal and the size was between 10 nm and 150 nm as shown in *Fig. 7*. The results carried out with AFM confirmed findings of SEM as shown in *Fig. 8*.

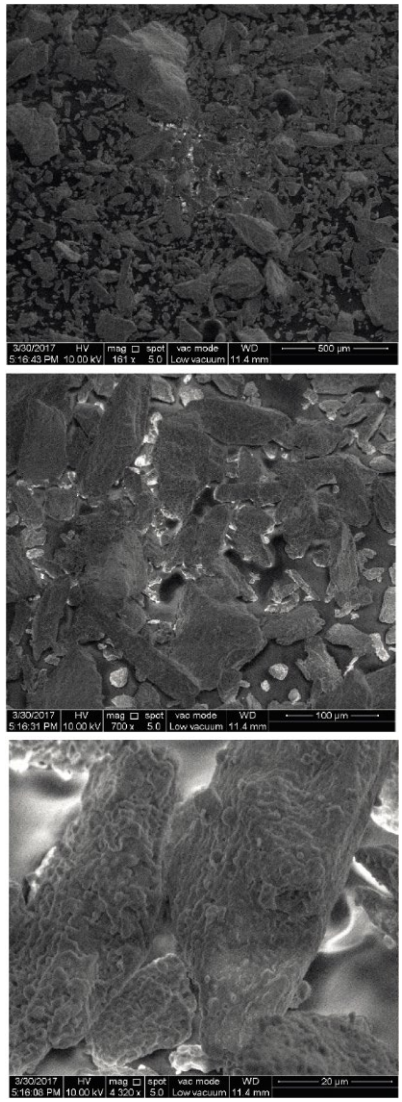

Fig. 6 SEM micrograph of bovine bone heated at 1000 °C showing the shape of HAp particles at three different magnifications
6. ábra SEM felvételek az 1000 °C-on hevített szarvasmarha csont szelet Hap. szemcsékről három különböző nagyításban

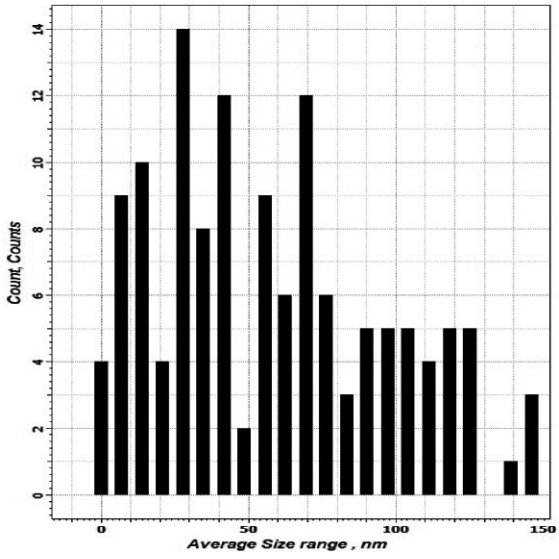

Fig. 7 Particle size of powder bone after heating at 1000 °C
7. ábra 1000 °C-os hevítés után szarvasmarha csont szemcsék mérete

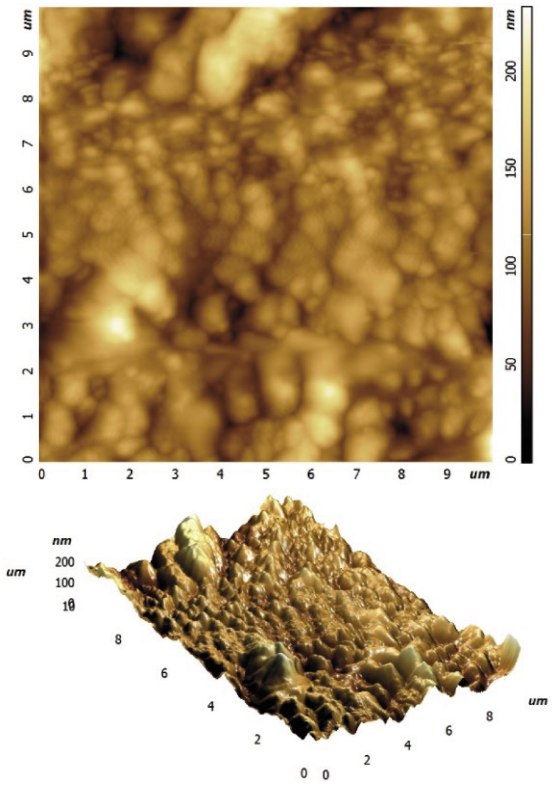

Fig. 8 Topography and surface properties of powder bone after heating at 1000 °C
8. ábra 1000 °C-on hevített szarvasmarha csont por topográfiai és felületi jellemzői

4. Conclusions

1- The result of EDS referred to the best calcination temperature for this study was 1000 °C due to Ca/P atomic ratio at this temperature was 1.6 that has been near stoichiometric hydroxyapatite (1.67) in human body.

2- FTIR and Raman analysis confirmed the formation of HAp by the presence of peaks matching to phosphate and hydroxyl groups which are of great significance in a scope of HAp structure.

3- The shape of HAp particles was irregular like needle and polygonal and the size was between 10 nm and 150 nm.

5. Acknowledgement

The authors would like to thank Dr. **Ali S. Hammood** and Ms. **Sora S. Hassan** (Materials Engineering Department, Faculty of Engineering, University of Kufa, Najaf, Iraq) for their support.

References

[1] Sobczak-kupiec, A., Pluta, K., & Malina, D. (2017). Studies on Bone-Derived Calcium Phosphate Materials. Journal of Renewable Materials, 5(3–4), 180–188. https://doi.org/10.7569/JRM.2017.634106

[2] Mucalo, M. (2015). Hydroxyapatite (HAp) for Biomedical Applications. Elsevier Ltd.

[3] Bose, S., & Tarafder, S. (2012). Calcium phosphate ceramic systems in growth factor and drug delivery for bone tissue engineering : A review. Acta Biomaterialia, 8(4), 1401–1421. https://doi.org/10.1016/j.actbio.2011.11.017

[4] Akram, M., & Ahmed, R. (2014). Extracting hydroxyapatite and its precursors from natural resources. Journal of Materials Science, 49(4), 1461–1475. https://doi.org/10.1007/s10853-013-7864-x

[5] Murugan, R., & Ramakrishna, S. (2005). Development of nanocomposites for bone grafting. Composites Science and Technology, 65, 2385–2406. https://doi.org/10.1016/j.compscitech.2005.07.022

[6] Mobasherpour, I., Heshajin, M. S., Kazemzadeh, A., & Zakeri, M. (2007). Synthesis of nanocrystalline hydroxyapatite by using precipitation method. Journal of Alloys and Compounds. https://doi.org/10.1016/j.jallcom.2006.05.018

[7] Sanosh, K. P., Chu, M. C., Balakrishnan, A., Kim, T. N., & Cho, S. J. (2009). Preparation and characterization of nano-hydroxyapatite powder using sol-gel technique. Bulletin of Materials Science. https://doi.org/10.1007/s12034-009-0069-x

[8] Hammood, A. S., Hassan, S. S., & Alkhafagy, M. T. (2017). Access to Optimal Calcination Temperature for Nanoparticle Synthesis from Hydroxyapatite Bovine Femur Bone Waste. Nano Biomedicine and Engineering, 9(3), 228–235. https://doi.org/10.5101/nbe.v9i3.p228-235

[9] Hammood, A. S., Hassan, S. S., & Alkhafagy, M. T. (2019). Comparison of Natural and Nano-synthetically-Produced Hydroxyapatite Powder. The Journal of The Minerals, Metals & Materials Society, 71(1), 272–278. https://doi.org/10.1007/s11837-018-3185-5

[10] Chen, B. H., Chen, K. I., Ho, M. L., Chen, H. N., Chen, W. C., & Wang, C. K. (2009). Synthesis of calcium phosphates and porous hydroxyapatite beads prepared by emulsion method. Materials Chemistry and Physics. https://doi.org/10.1016/j.matchemphys.2008.06.040

[11] Venkatesan, J., Lowe, B., Manivasagan, P., Kang, K. H., Chalisserry, E. P., Anil, S., … Kim, S. K. (2015). Isolation and characterization of nano-hydroxyapatite from salmon fish bone. Materials. https://doi.org/10.3390/ma8085253

[12] Terzioğlu, P., Öğüt, H., & Kalemtaş, A. (2018). Natural calcium phosphates from fish bones and their potential biomedical applications. Materials Science and Engineering C. https://doi.org/10.1016/j.msec.2018.06.010

[13] Jaber, H. L., Hammood, A. S., & Parvin, N. (2018). Synthesis and characterization of hydroxyapatite powder from natural Camelus bone. Journal of the Australian Ceramic Society, 54(1), 1–10. https://doi.org/10.1007/s41779-017-0120-0

[14] Hassanen, J., & Tunde, K. (2019). Selective laser melting of Ti alloys and hydroxyapatite for tissue engineering: progress and challenges. Materials Research Express. https://doi.org/10.1088/2053-1591/ab1dee

[15] Piccirillo, C., Silva, M. F., Pullar, R. C., Braga Da Cruz, I., Jorge, R., Pintado, M. M. E., & Castro, P. M. L. (2013). Extraction and characterisation of apatite- and tricalcium phosphate-based materials from cod fish bones. Materials Science and Engineering C, 33(1), 103–110. https://doi.org/10.1016/j.msec.2012.08.014

[16] Sobczak-Kupiec, A., Kijkowska, R., & Malina, D. (2016). Infusion of Ag-Ion from Aqueous Solution into Solid Calcium Phosphate of Hydroxyapatite (HA) Crystal Structure. Journal of the American Ceramic Society, 99(9), 3129–3135. https://doi.org/10.1111/jace.14317

[17] Ślósarczyk, A., Paszkiewicz, Z., & Paluszkiewicz, C. (2005). FTIR and XRD evaluation of carbonated hydroxyapatite powders synthesized by wet methods. Journal of Molecular Structure, 744–747(SPEC. ISS.), 657–661. https://doi.org/10.1016/j.molstruc.2004.11.078

[18] Sofronia, A. M., Baies, R., Anghel, E. M., Marinescu, C. A., & Tanasescu, S. (2014). Thermal and structural characterization of synthetic and natural nanocrystalline hydroxyapatite. Materials Science and Engineering C, 43, 153–163. https://doi.org/10.1016/j.msec.2014.07.023

Ref.:
Jaber, Hassanen L. – **Kovács**, Tünde Anna: *Preparation and synthesis of hydroxyapatite bio-ceramic from bovine bone by thermal heat treatment*
Építőanyag – Journal of Silicate Based and Composite Materials, Vol. 71, No. 3 (2019), 98–101. p.
https://doi.org/10.14382/epitoanyag-jsbcm.2019.18

15TH INTERNATIONAL CONGRESS ON THE CHEMISTRY OF CEMENT

ICCC PRAGUE 2019

The ICCC 2019 will present cement and environmental development worldwide and renowned experts from all over the world are invited to present their work at the Congress. The scientific programme will cover the topics of the newest and the most important research and development describing cement and clinker chemistry (incl. kiln process technology), the nano and macro properties of the clinker and cement, hydration processes, the impact of additives and admixtures, leaching processes, the behaviour of trace elements, microscopy outputs, alternative binders, durability of concrete, standards and codes, as well as modern laboratory instrument equipment. The Congress will consist of many plenary lectures and parallel sessions on a variety of topics, offering to the scientists, researchers, producers and users from all over the world the opportunity to meet, to present and to exchange their research results and knowledge.

September 16–20, 2019

www.iccc2019.org

About EGU

EGU, the European Geosciences Union, is Europe's premier geosciences union, dedicated to the pursuit of excellence in the Earth, planetary, and space sciences for the benefit of humanity, worldwide. It was established in September 2002 as a merger of the European Geophysical Society (EGS) and the European Union of Geosciences (EUG), and has headquarters in Munich, Germany.

It is a non-profit international union of scientists with about 15,000 members from all over the world. Membership is open to individuals who are professionally engaged in or associated with geosciences and planetary and space sciences and related studies, including students and retired seniors.

The EGU publishes a number of diverse scientific journals, which use an innovative open access format, and organises a number of topical meetings, and education and outreach activities. It also honours scientists with a number of awards and medals. The annual EGU General Assembly is the largest and most prominent European geosciences event, attracting over 14,000 scientists from all over the world in recent years. The meeting's sessions cover a wide range of topics, including volcanology, planetary exploration, the Earth's internal structure and atmosphere, climate, as well as energy and resources.

www.egu.eu

GUIDELINE FOR AUTHORS

The manuscript must contain the followings: title; author's name, workplace, e-mail address; abstract, keywords; main text; acknowledgement (optional)**; references; figures, photos with notes; tables with notes; short biography** (information on the scientific works of the authors).

The full manuscript should not be more than 6 pages including figures, photos and tables. Settings of the word document are: 3 cm margin up and down, 2,5 cm margin left and right. Paper size: A4. Letter size 10 pt, type: Times New Roman. Lines: simple, justified.

TITLE, AUTHOR

The title of the article should be short and objective.

Under the title the name of the author(s), workplace, e-mail address.

If the text originally was a presentation or poster at a conference, it should be marked.

ABSTRACT, KEYWORDS

The abstract is a short summary of the manuscript, about a half page size. The author should give keywords to the text, which are the most important elements of the article.

MAIN TEXT

Contains: materials and experimental procedure (or something similar), results and discussion (or something similar), conclusions.

REFERENCES

References are marked with numbers, e.g. [6], and a bibliography is made by the reference's order. References should be provided together with the DOI if available.

Examples:

Journals:

[6] Mohamed, K. R. – El-Rashidy, Z. M. – Salama, A. A.: In vitro properties of nano-hydroxyapatite/chitosan biocomposites. *Ceramics International.* 37(8), December 2011, pp. 3265–3271, http://doi.org/10.1016/j.ceramint.2011.05.121

Books:

[6] Mehta, P. K. – Monteiro, P. J. M.: Concrete. Microstructure, properties, and materials. *McGraw-Hill*, 2006, 659 p.

FIGURES, TABLES

All drawings, diagrams and photos are figures. The **text should contain references to all figures and tables**. This shows the place of the figure in the text. Please send all the figures in attached files, and not as a part of the text. **All figures and tables should have a title**.

Authors are asked to submit color figures by submission. Black and white figures are suggested to be avoided, however, acceptable.

The figures should be: tiff, jpg or eps files, 300 dpi at least, photos are 600 dpi at least.

BIOGRAPHY

Max. 500 character size professional biography of the author(s).

CHECKING

The editing board checks the articles and informs the authors about suggested modifications. Since the author is responsible for the content of the article, the author is not liable to accept them.

CONTACT

Please send the manuscript in electronic format to the following e-mail address: femgomze@uni-miskolc.hu and epitoanyag@szte.org.hu or by post: Scientific Society of the Silicate Industry, Budapest, Bécsi út 122–124., H-1034, HUNGARY

We kindly ask the authors to give their e-mail address and phone number on behalf of the quick conciliation.

Építőanyag – *Journal of Silicate Based and Composite Materials*, Quarterly peer-reviewed periodical of the Hungarian Scientific Society of the Silicate Industry, SZTE.
http://epitoanyag.org.hu

ESCM
EUROPEAN SOCIETY FOR COMPOSITE MATERIALS

THE SCIENTIFIC, ENGIEERING AND INDUSTRIAL COMMNITY INVOLVED WITH COMPOSITE MATERIALS

THE SOCIETY

OBJECTIVES OF THE SOCIETY

ESCM is a European, non-governmental, non-profit scientific and engineering organisation with the following objectives:

- To encourage the free interchange of information on all those aspects related to composite materials which of are interest to the scientific and engineering community.
- To provide a Europe-wide forum for the discussion of such topics, e.g. by organising the ECCM (European Conference on Composite Materials) and more specialised symposia related to composites.
- To guide and foster the understanding and utilisation of the science and technology of composite materials.
- To promote European co-operation in the study of topics in composite materials science and technology.
- To promote liaison with engineering and scientific bodies throughout Europe with similar aims and to serve as a facilitator for communication between such bodies.
- To foster an environment for timely and cost-effective research, development and implementation of advanced technology in composites.
- To encourage the education of young specialists in the disciplines supporting composite materials science and technology.
- To recognise individuals of outstanding achievement in the science, technology, engineering, and application of composite materials.

CES - SILICONES EUROPE

SILICONES & YOU

Silicones have literally thousands of applications that collectively bring safety, comfort and enjoyment to life. They improve the performance and reliability of millions of modern products.

THE SCIENCE

Silicones chemistry is one of the most versatile chemistries on the planet, rendering it full of possibilities and producing a wide range of formulations and uses from aesthetic to technical.

WHO IS CES?

We are a non-profit organisation representing all major producers of silicones in Europe. We provide information on silicones from a health, safety and environmental perspective.

WWW.SILICONES.EU